

Supporting Information For:

**Synthesis and Characterization of**  
**Potassium Aryl- and Alkyl-Substituted Silylchalcogenolate Ligands**

Jessie L. Brown,<sup>a,c</sup> Ashley C. Montgomery,<sup>c</sup> Christopher A. Samaan,<sup>c</sup> Michael T. Janicke,<sup>a</sup> Brian  
L. Scott<sup>b</sup> and Andrew J. Gaunt<sup>\*,a</sup>

<sup>a</sup>Chemistry Division and <sup>b</sup>Materials Physics and Applications Division, Los Alamos National  
Laboratory, Los Alamos, New Mexico 87545, USA

<sup>c</sup>Chemistry Department, Natural Sciences and Mathematics Division, Transylvania University,  
Lexington, Kentucky 40508, USA

\*To whom correspondence should be addressed. Email: [gaunt@lanl.gov](mailto:gaunt@lanl.gov)

## IR Spectra.

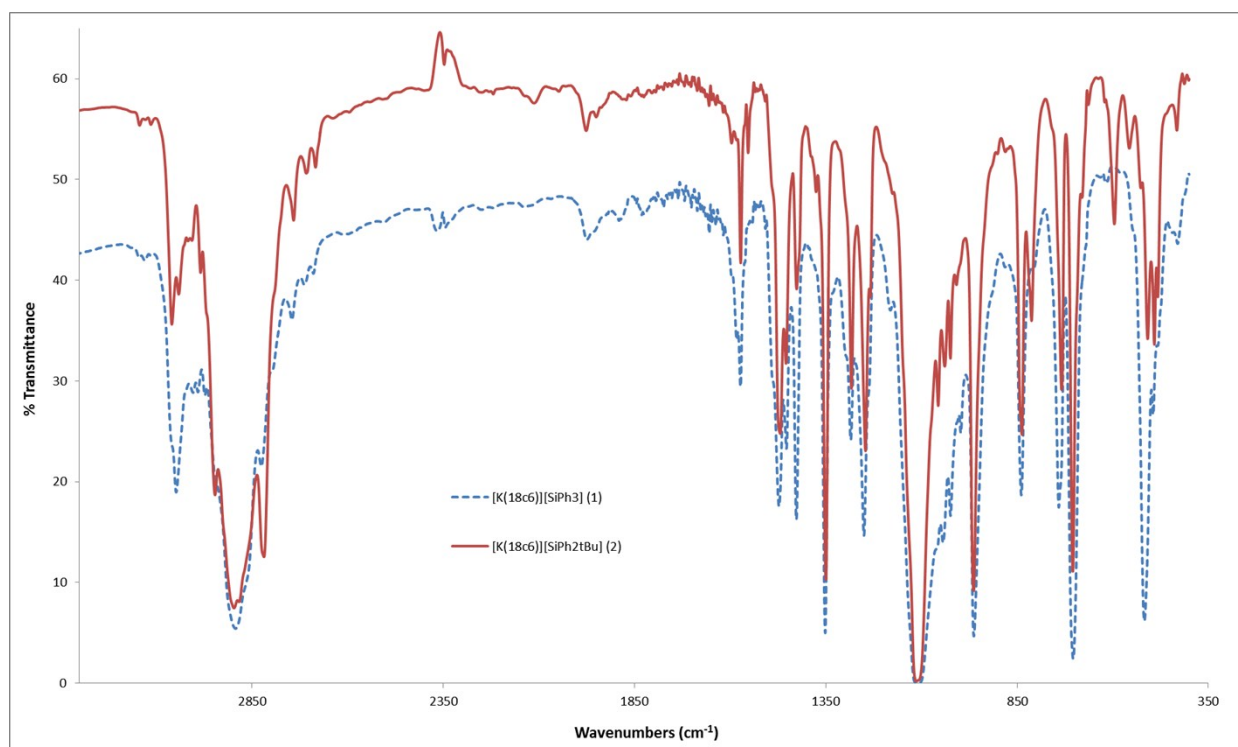


**Figure S1.** Overlay of IR spectra of **1** and **2** (KBr mull). The stretches observed from ~2400-2300 cm<sup>-1</sup> are persistent artifacts from the instrument that were not able to be subtracted from the background.

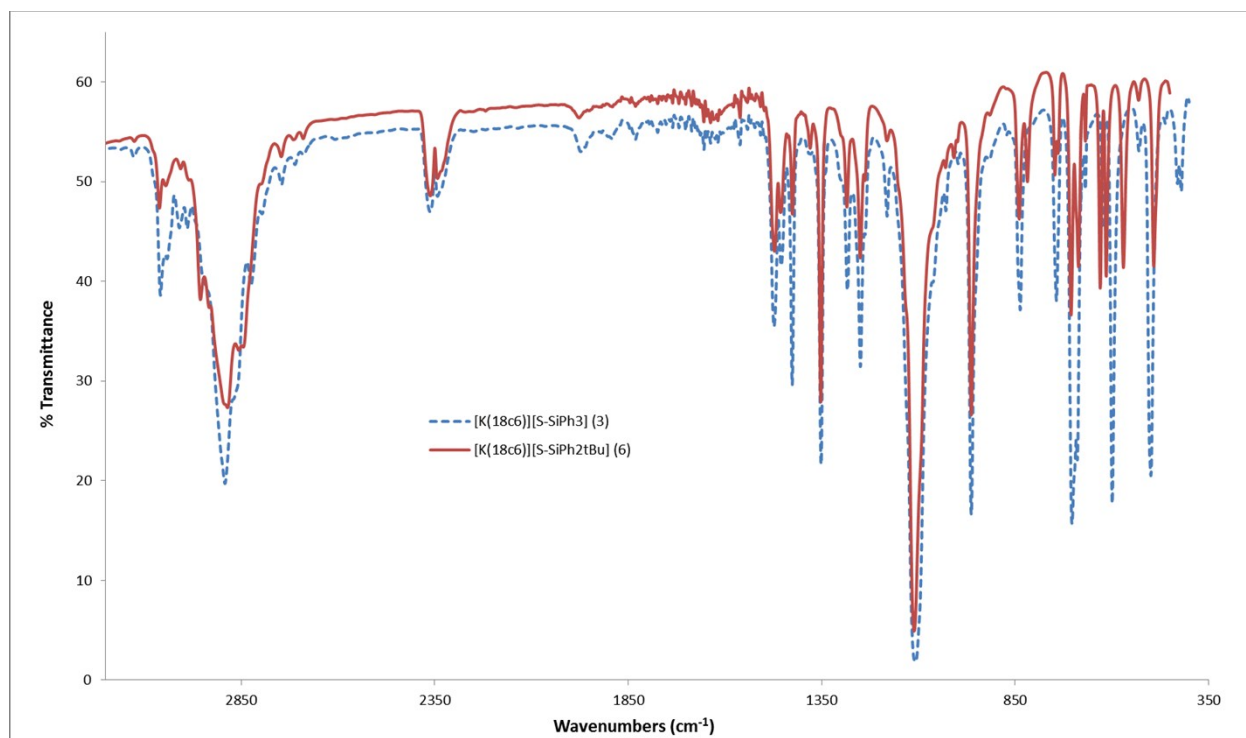


**Figure S2.** Overlay of IR spectra of **3** and **6** (KBr mull). The stretches observed from  $\sim 2400$ - $2300$   $\text{cm}^{-1}$  are persistent artifacts from the instrument that were not able to be subtracted from the background.

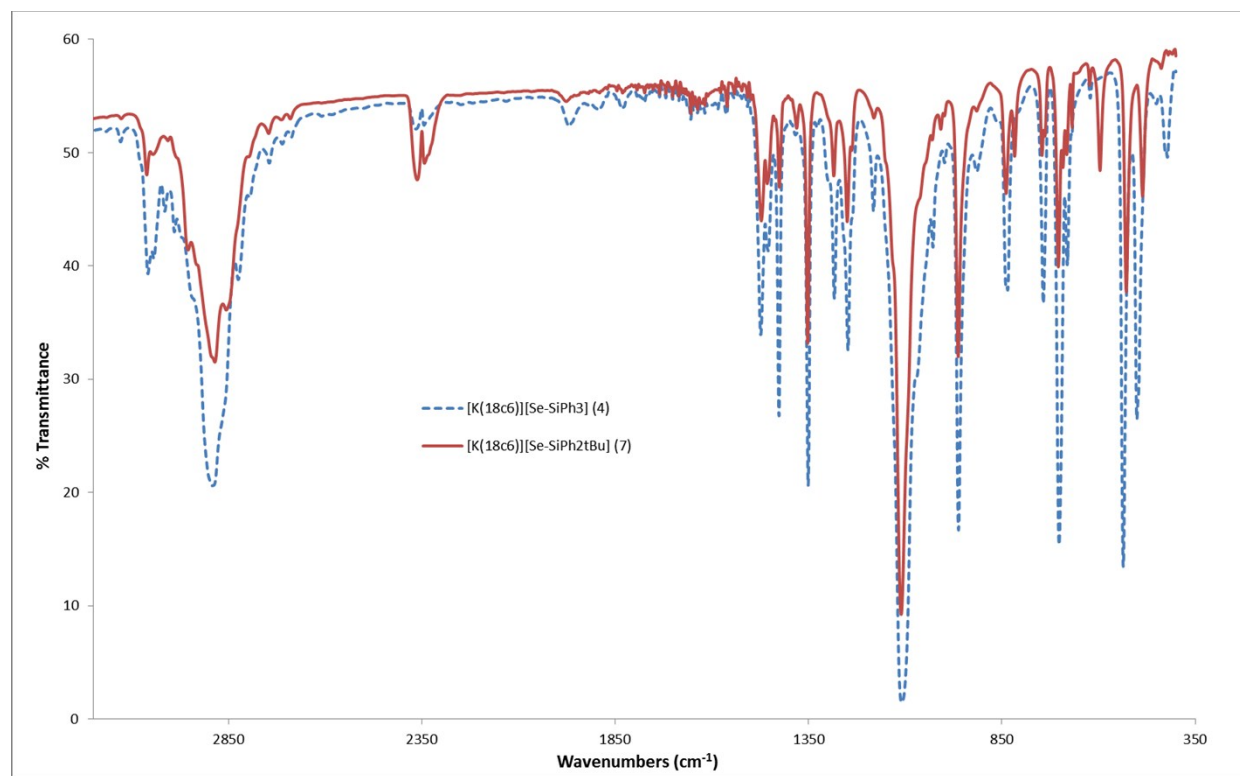


**Figure S3.** Overlay of IR spectra of **4** and **7** (KBr mull). The stretches observed from  $\sim 2400$ - $2300$   $\text{cm}^{-1}$  are persistent artifacts from the instrument that were not able to be subtracted from the background.

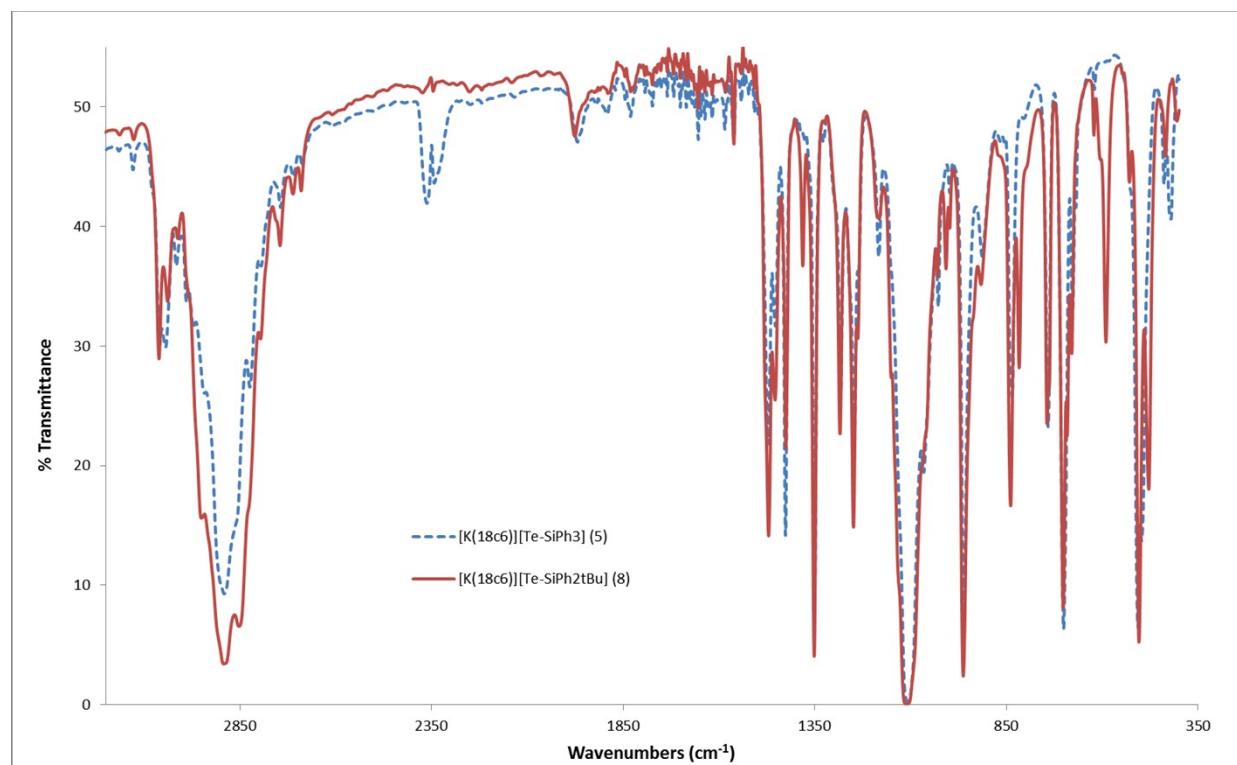


**Figure S4.** Overlay of IR spectra of **5** and **8** (KBr mull). The stretches observed from  $\sim 2400$ - $2300$   $\text{cm}^{-1}$  are persistent artifacts from the instrument that were not able to be subtracted from the background.

# NMR Spectra.

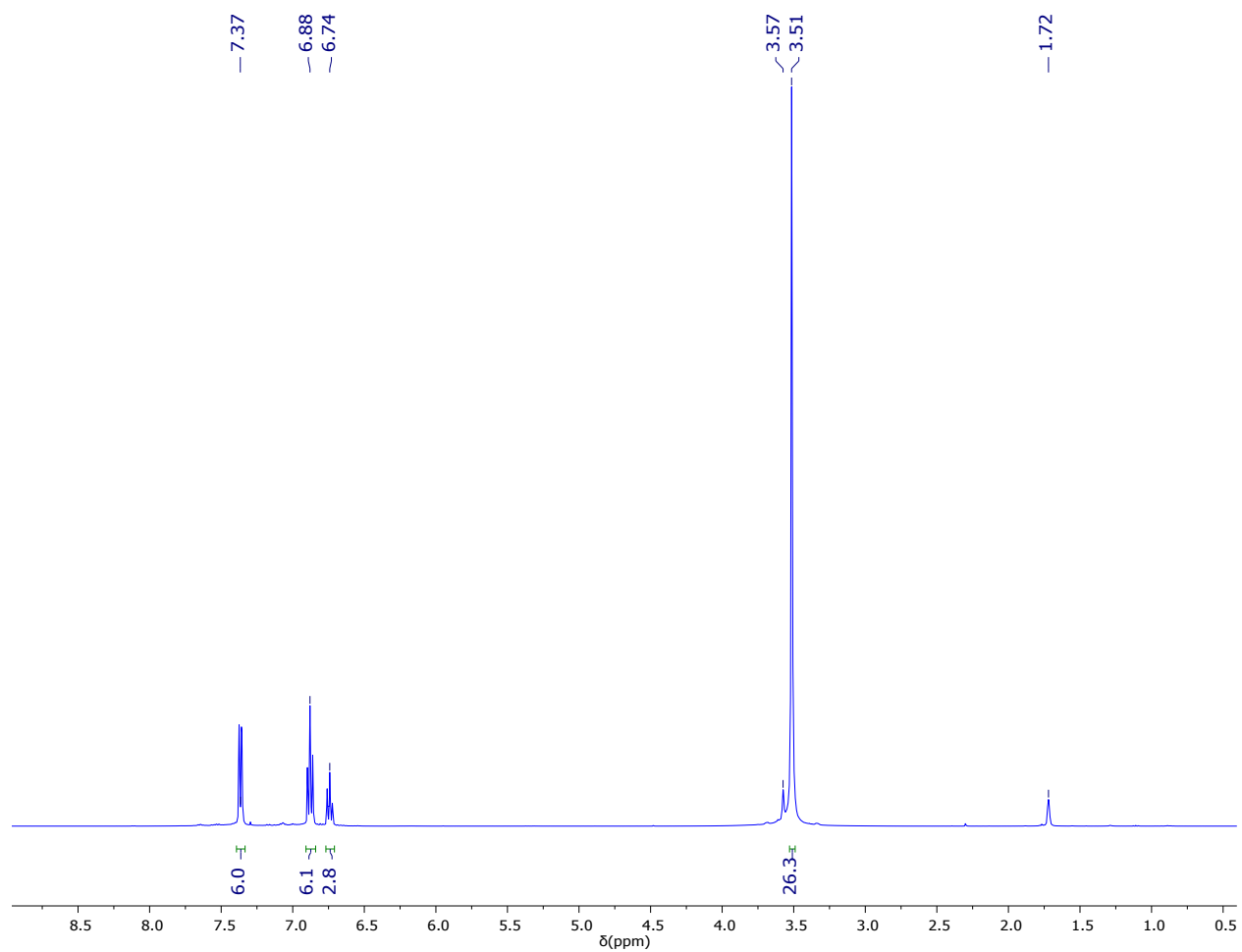


**Figure S5.**  $^1\text{H}$  NMR spectrum of **1** in  $\text{THF-}d_8$ .

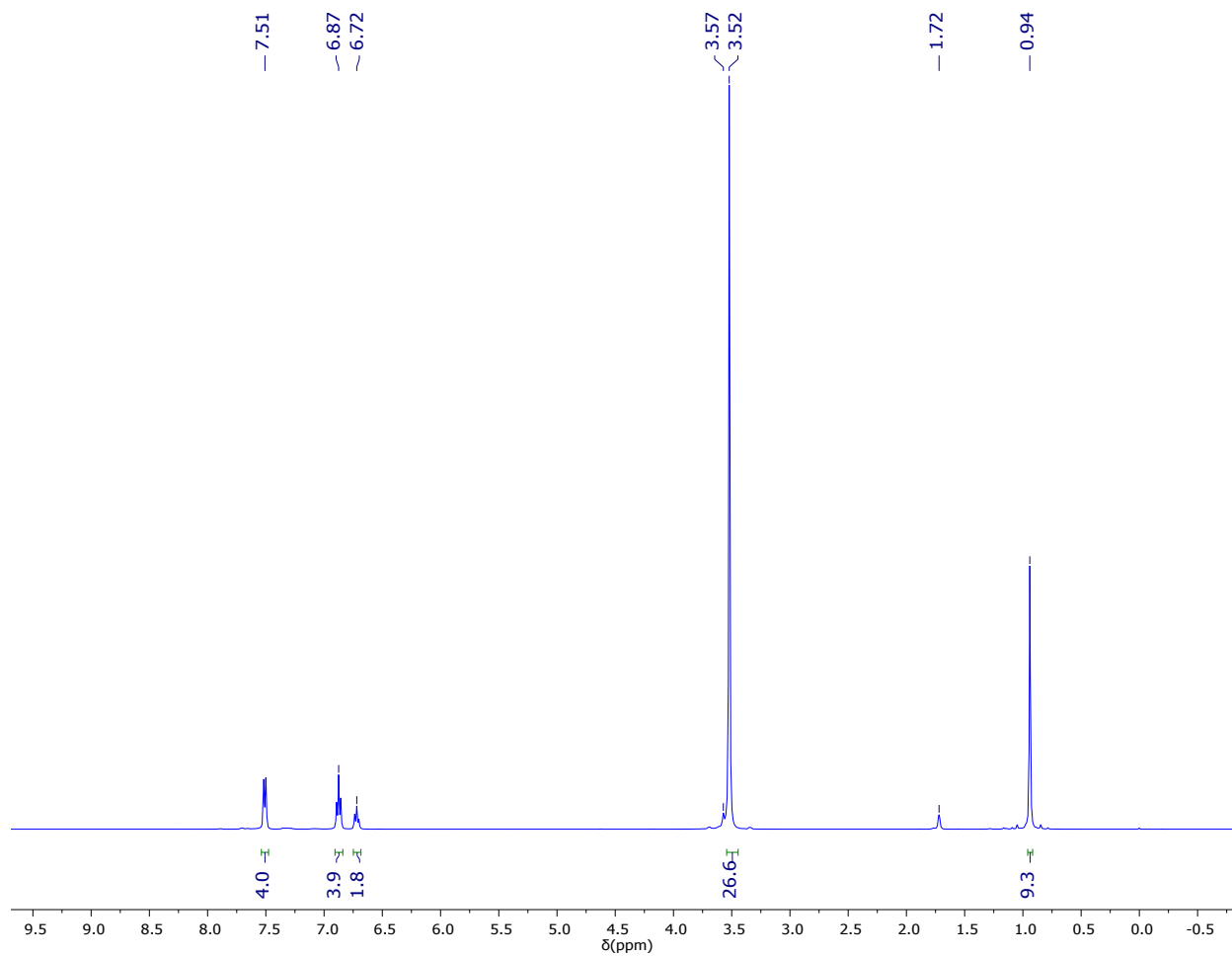


**Figure S6.**  $^1\text{H}$  NMR spectrum of **2** in  $\text{THF-}d_8$ .

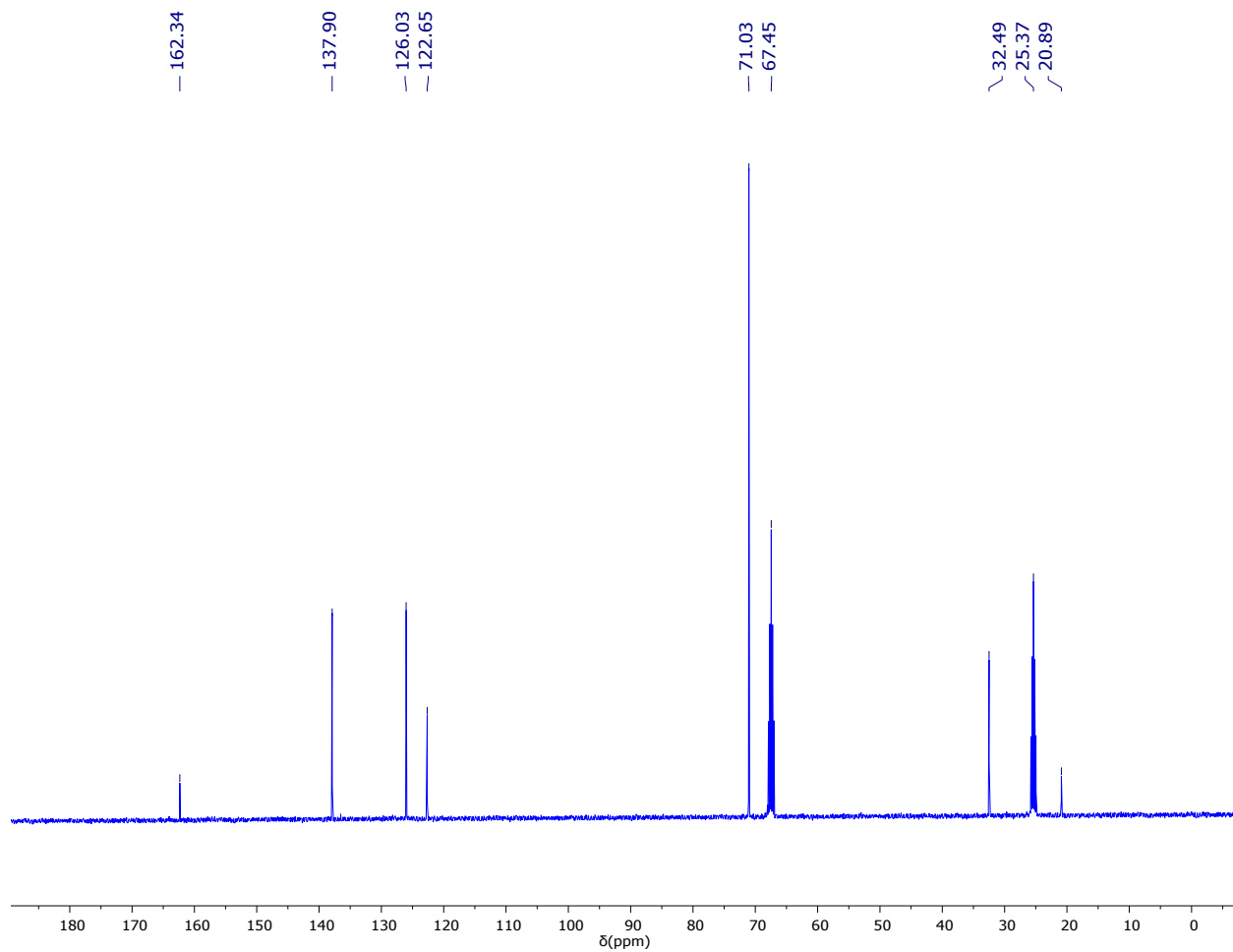


**Figure S7.**  $^{13}\text{C}$  NMR spectrum of **2** in  $\text{THF-}d_8$ .

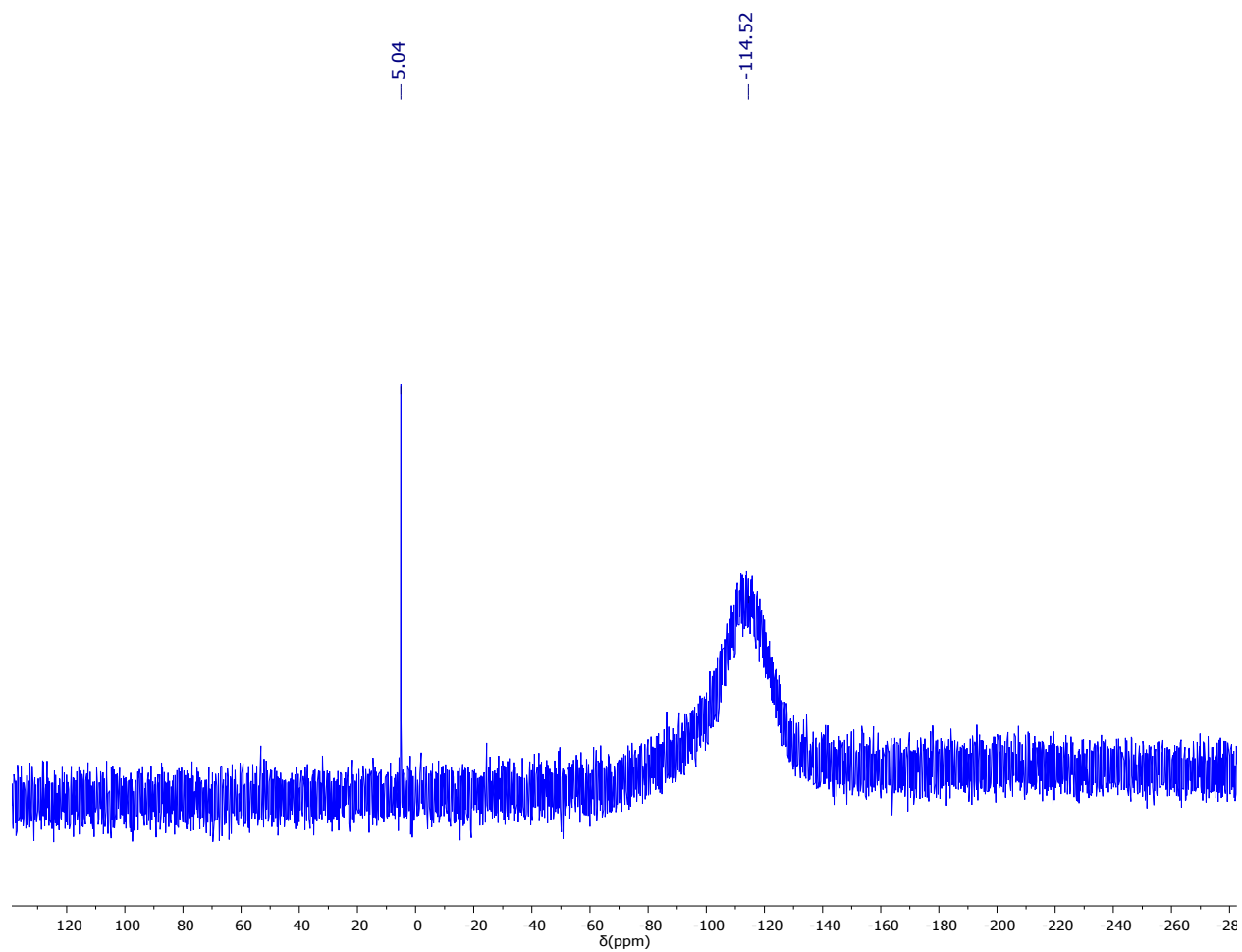


**Figure S8.**  $^{29}\text{Si}$  NMR spectrum of **2** in  $\text{THF-}d_8$ . The resonance at -114.52 ppm is assignable to the borosilicate glass from the NMR tube.

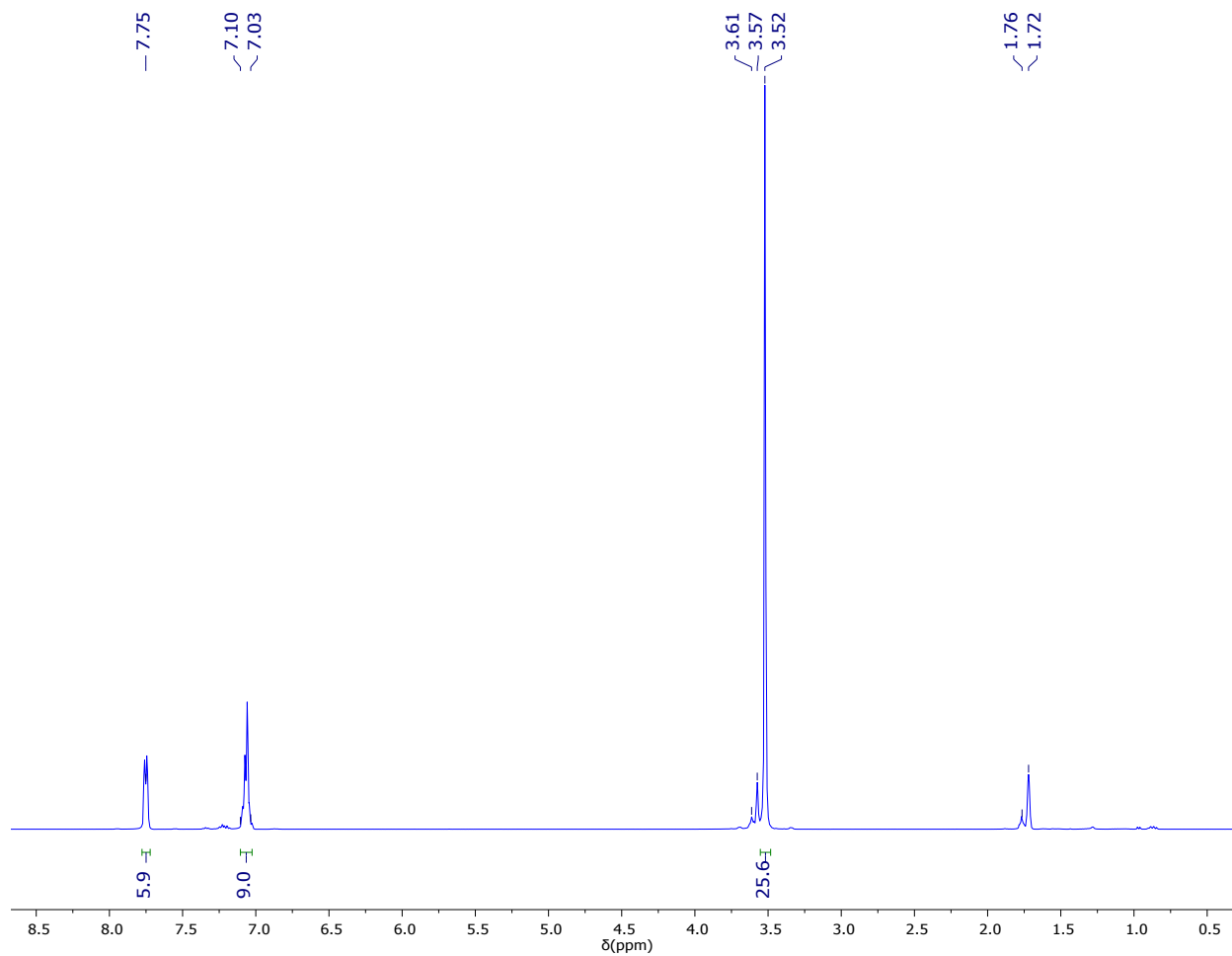


**Figure S9.**  $^1\text{H}$  NMR spectrum of **3** in  $\text{THF-}d_8$ .

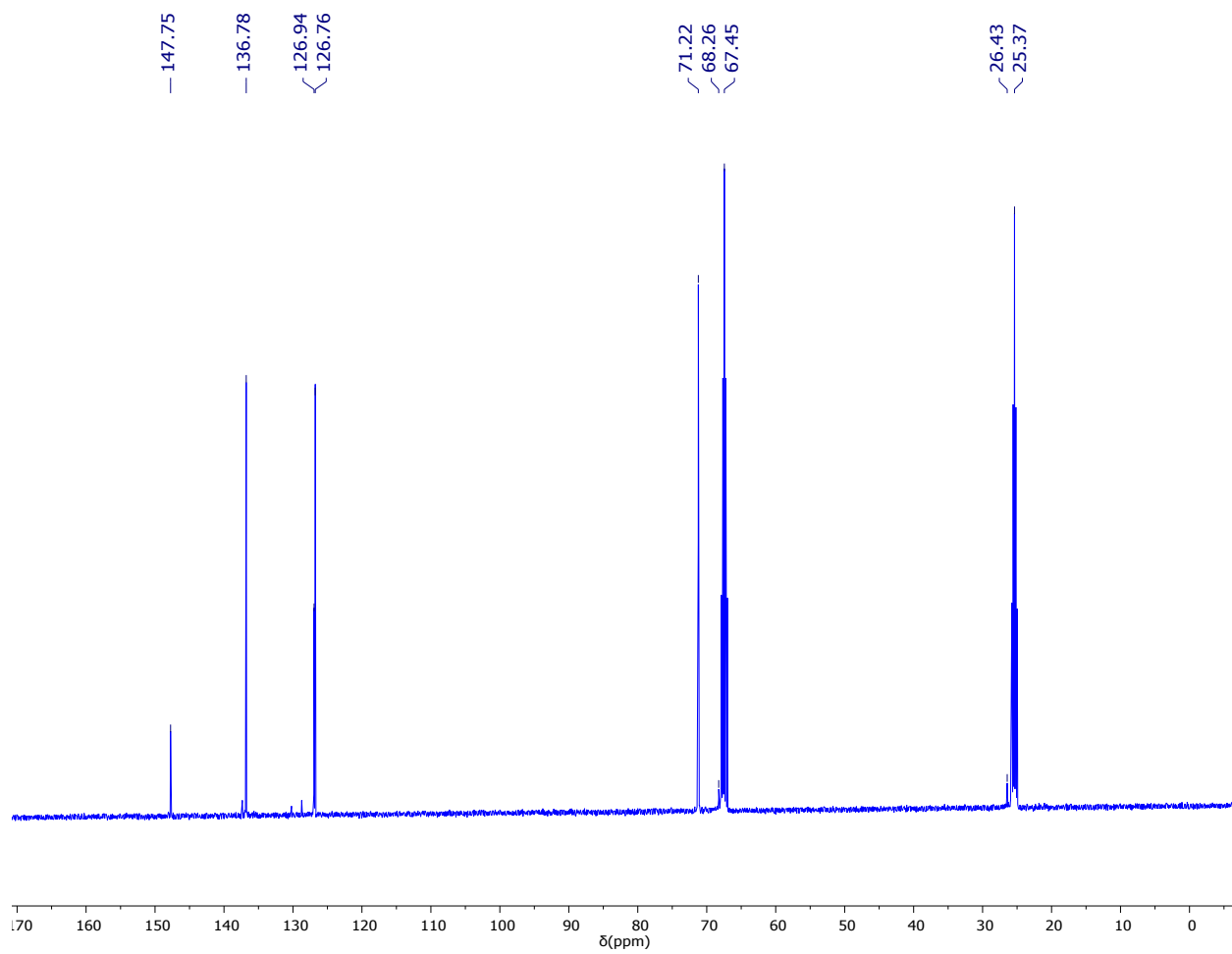


**Figure S10.**  $^{13}\text{C}$  NMR spectrum of **3** in  $\text{THF-}d_8$ .

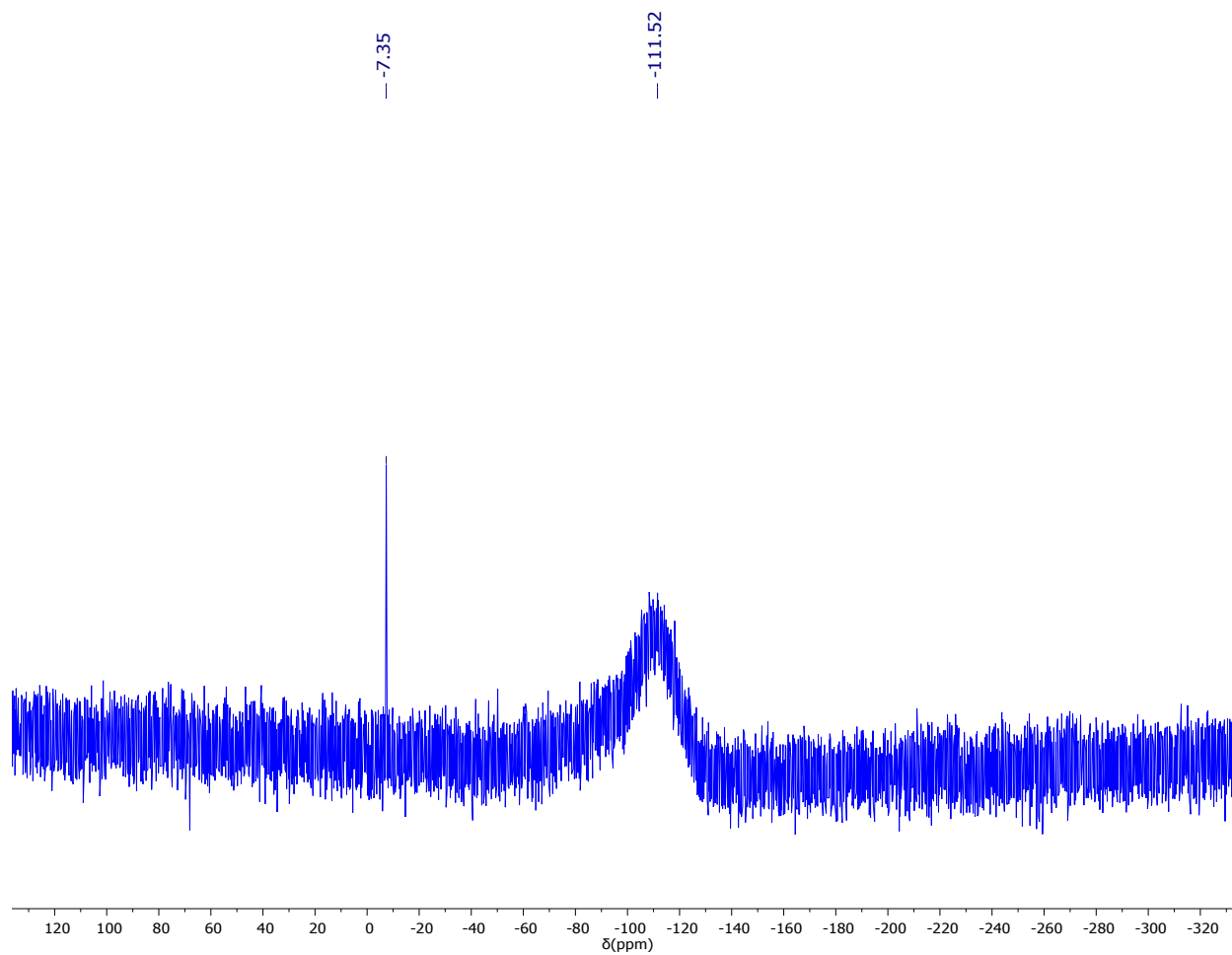


**Figure S11.**  $^{29}\text{Si}$  NMR spectrum of **3** in  $\text{THF-}d_8$ . The resonance at -111.52 ppm is assignable to the borosilicate glass from the NMR tube.

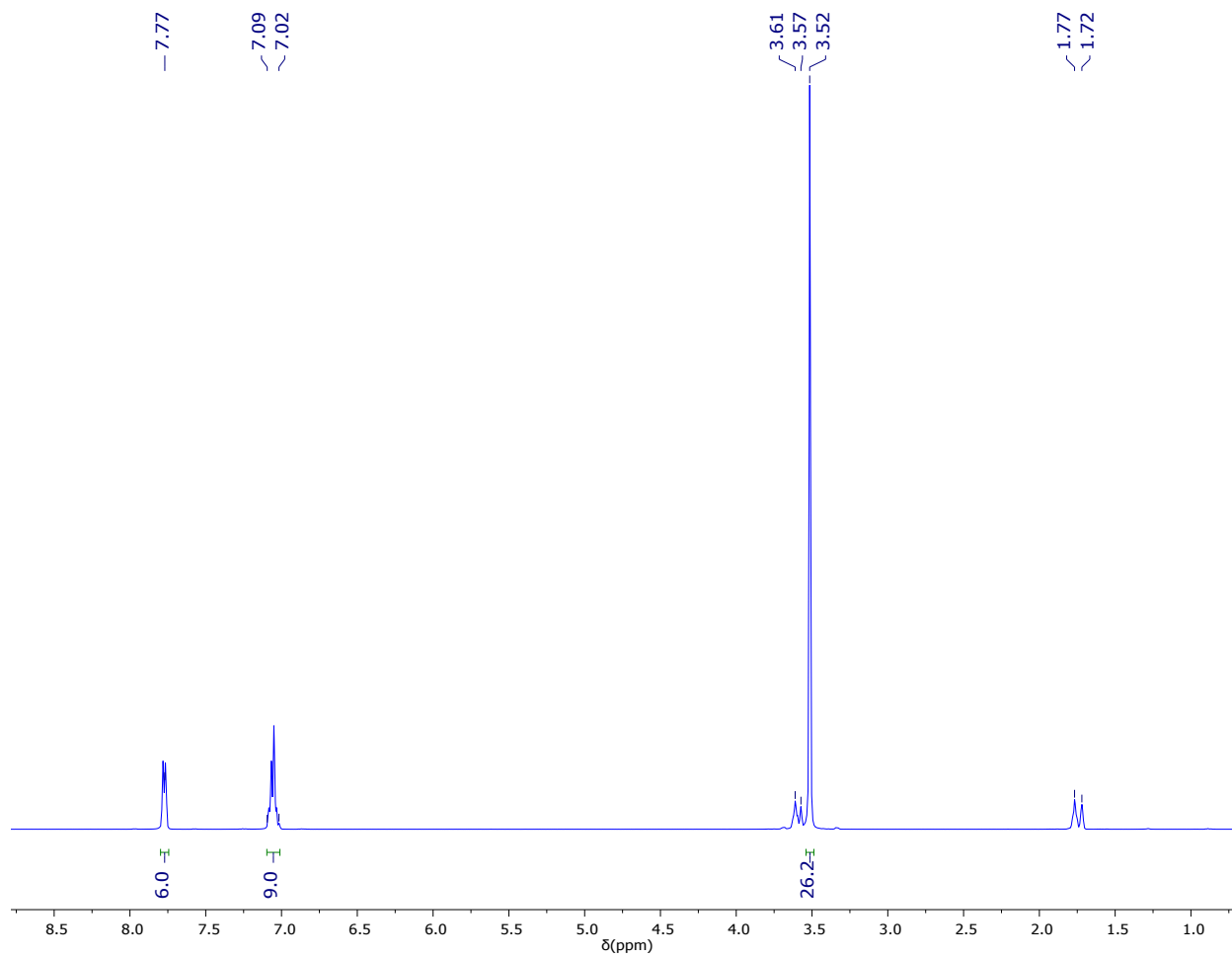


**Figure S12.**  $^1\text{H}$  NMR spectrum of **4** in  $\text{THF-}d_8$ .

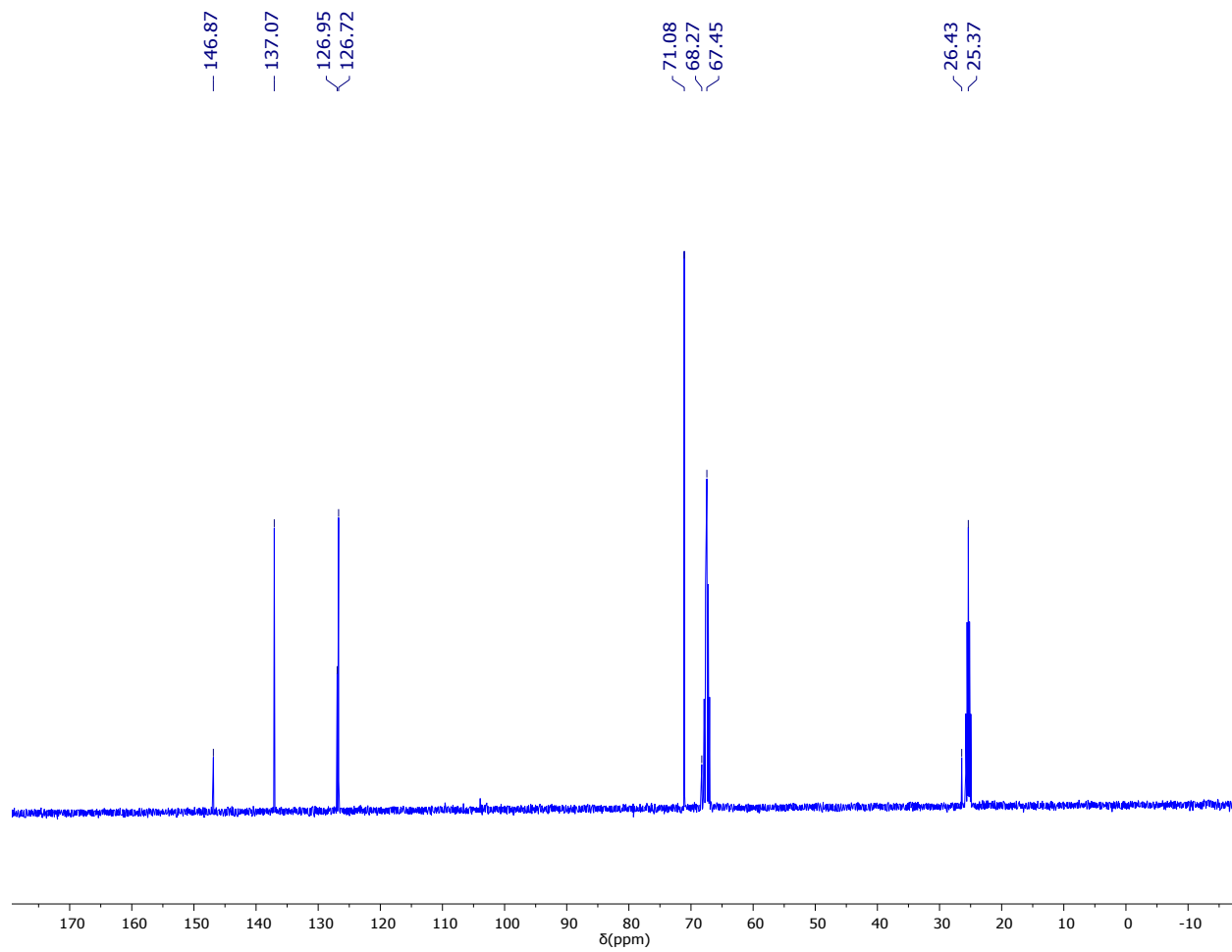


**Figure S13.**  $^{13}\text{C}$  NMR spectrum of **4** in  $\text{THF-}d_8$ .

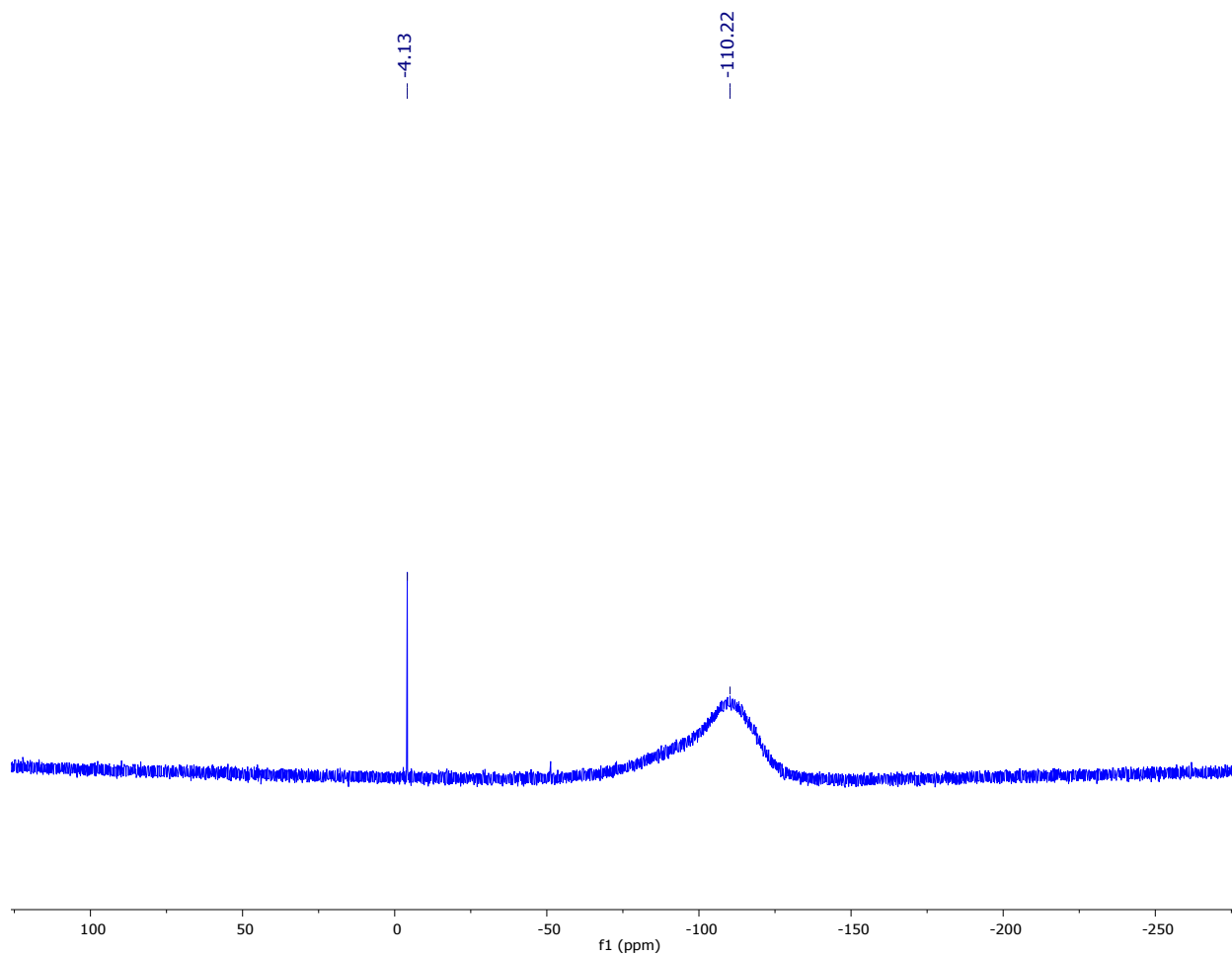


**Figure S14.**  $^{29}\text{Si}$  NMR spectrum of **4** in  $\text{THF-}d_8$ . The resonance at -110.22 ppm is assignable to the borosilicate glass from the NMR tube.

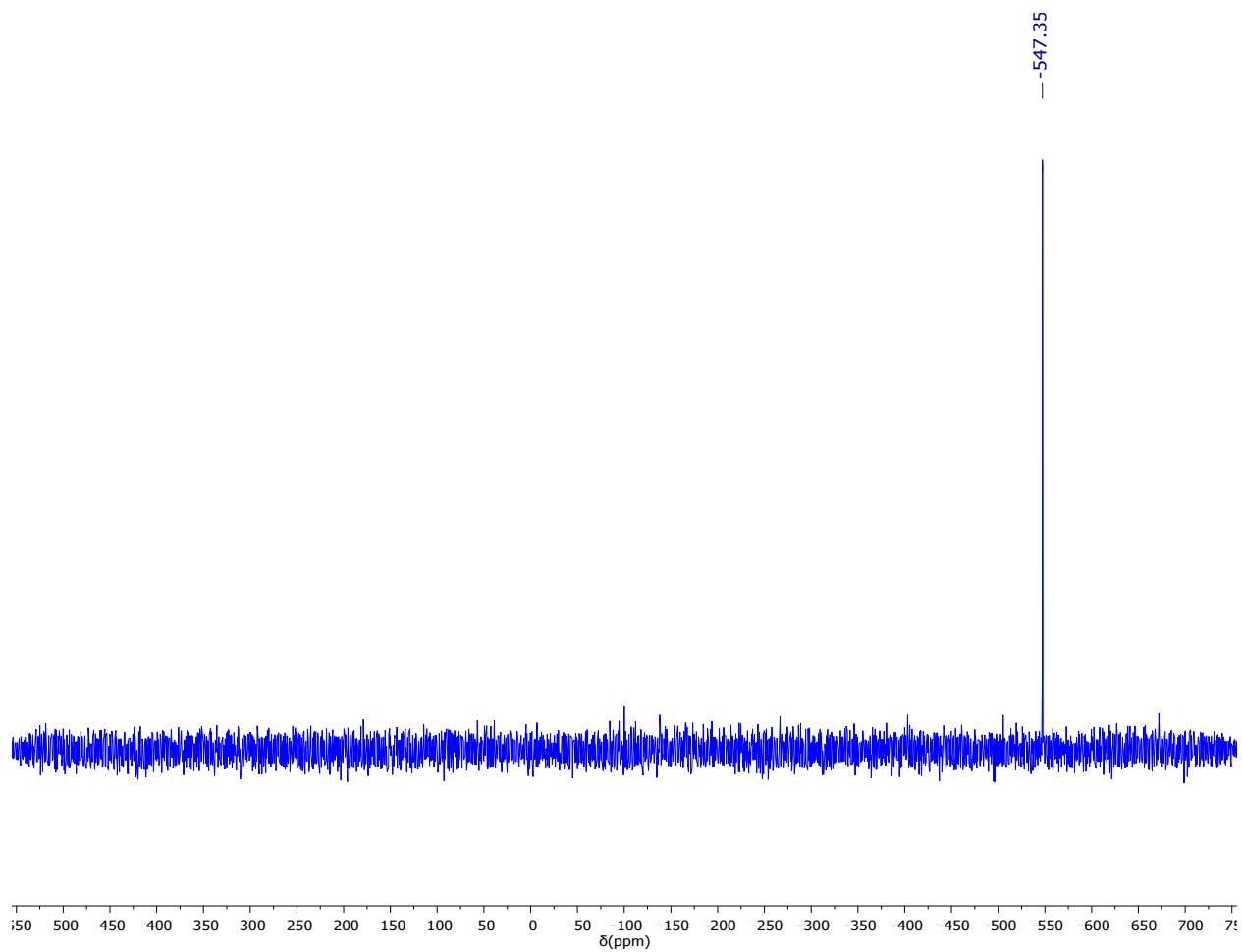


**Figure S15.**  $^{77}\text{Se}$  NMR spectrum of **4** in  $\text{THF-}d_8$ .

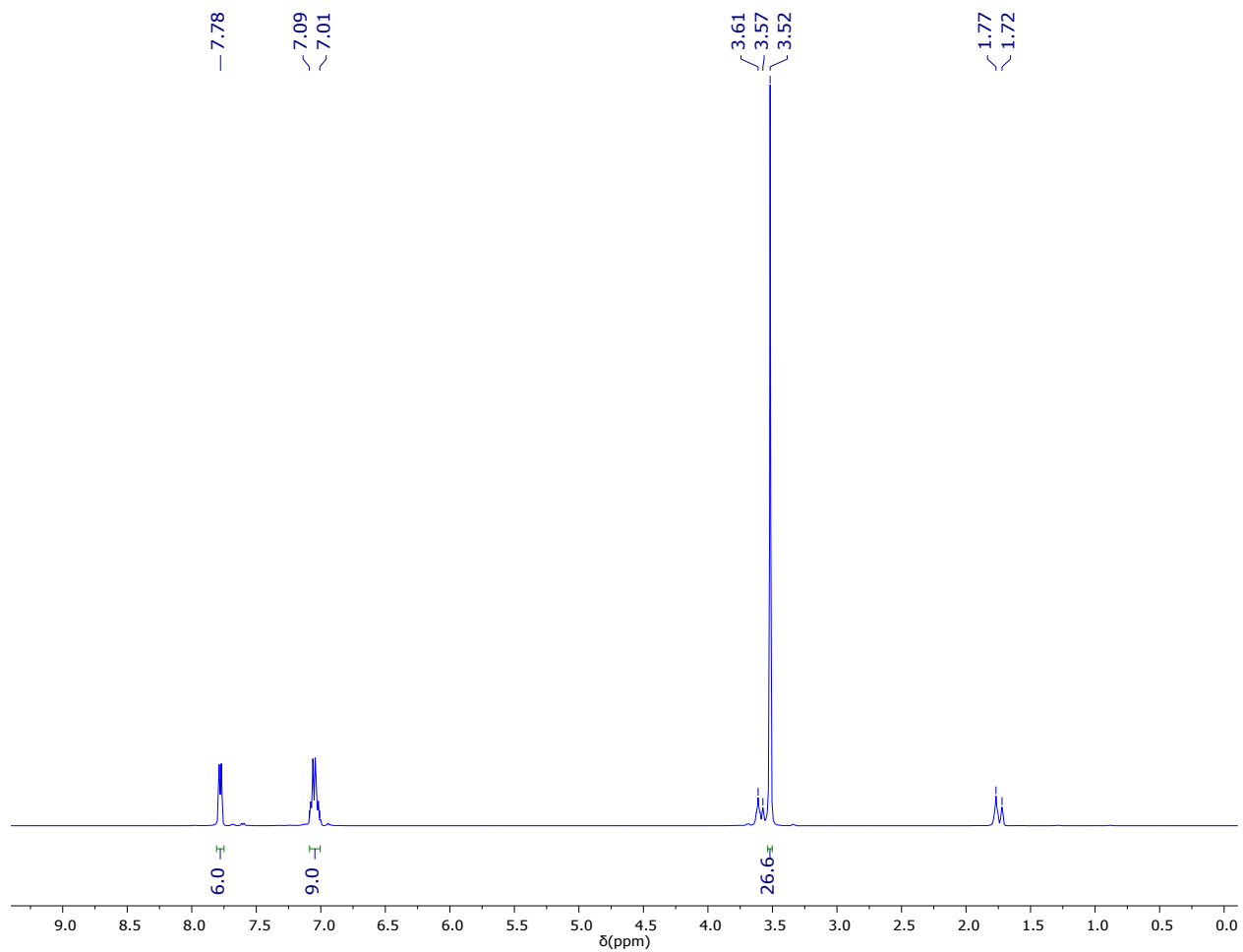


**Figure S16.**  $^1\text{H}$  NMR spectrum of **5** in  $\text{THF-}d_8$ .

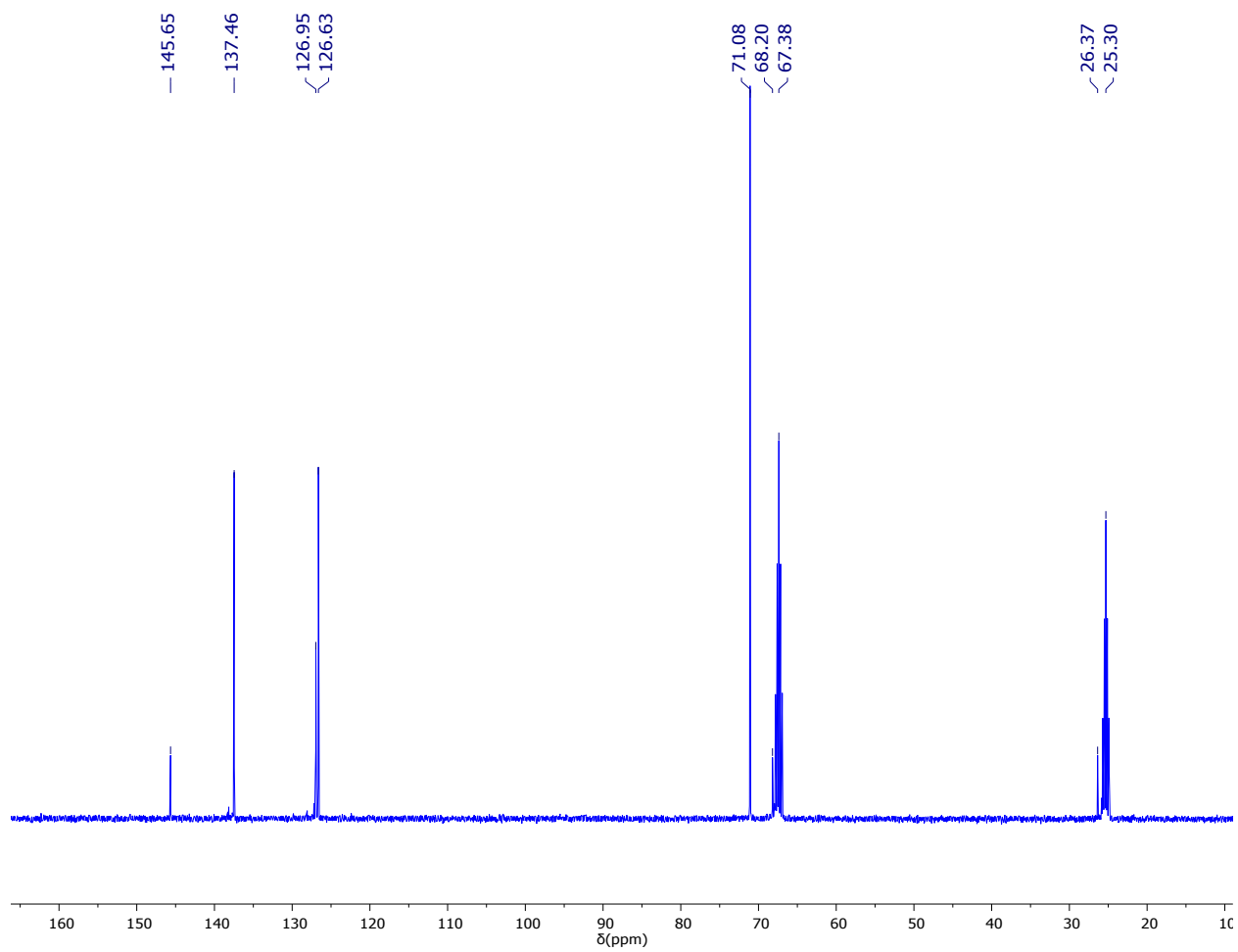


**Figure S17.**  $^{13}\text{C}$  NMR spectrum of **5** in  $\text{THF-}d_8$ .

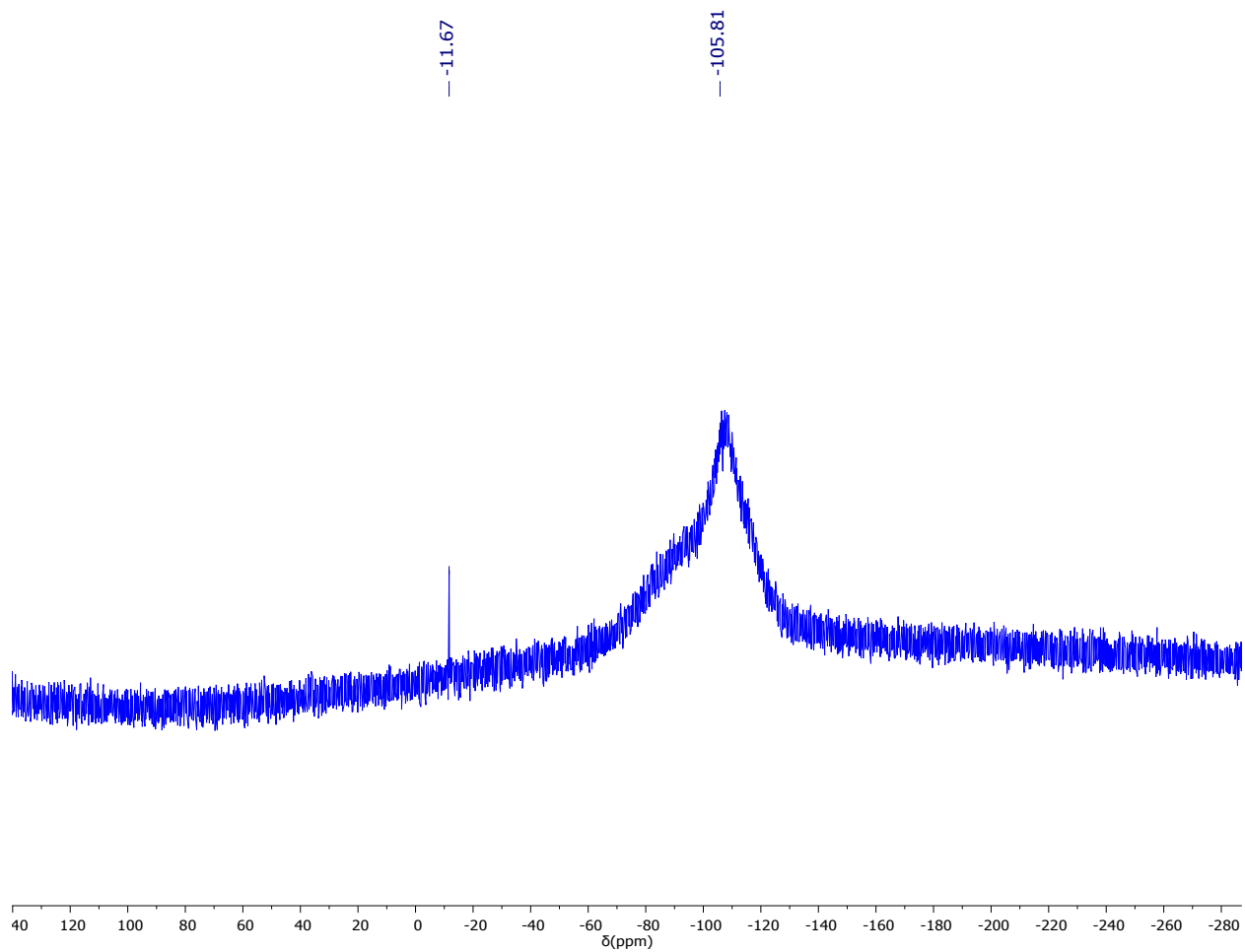


**Figure S18.**  $^{29}\text{Si}$  NMR spectrum of **5** in  $\text{THF-}d_8$ . The resonance at  $-105.81$  ppm is assignable to the borosilicate glass from the NMR tube.

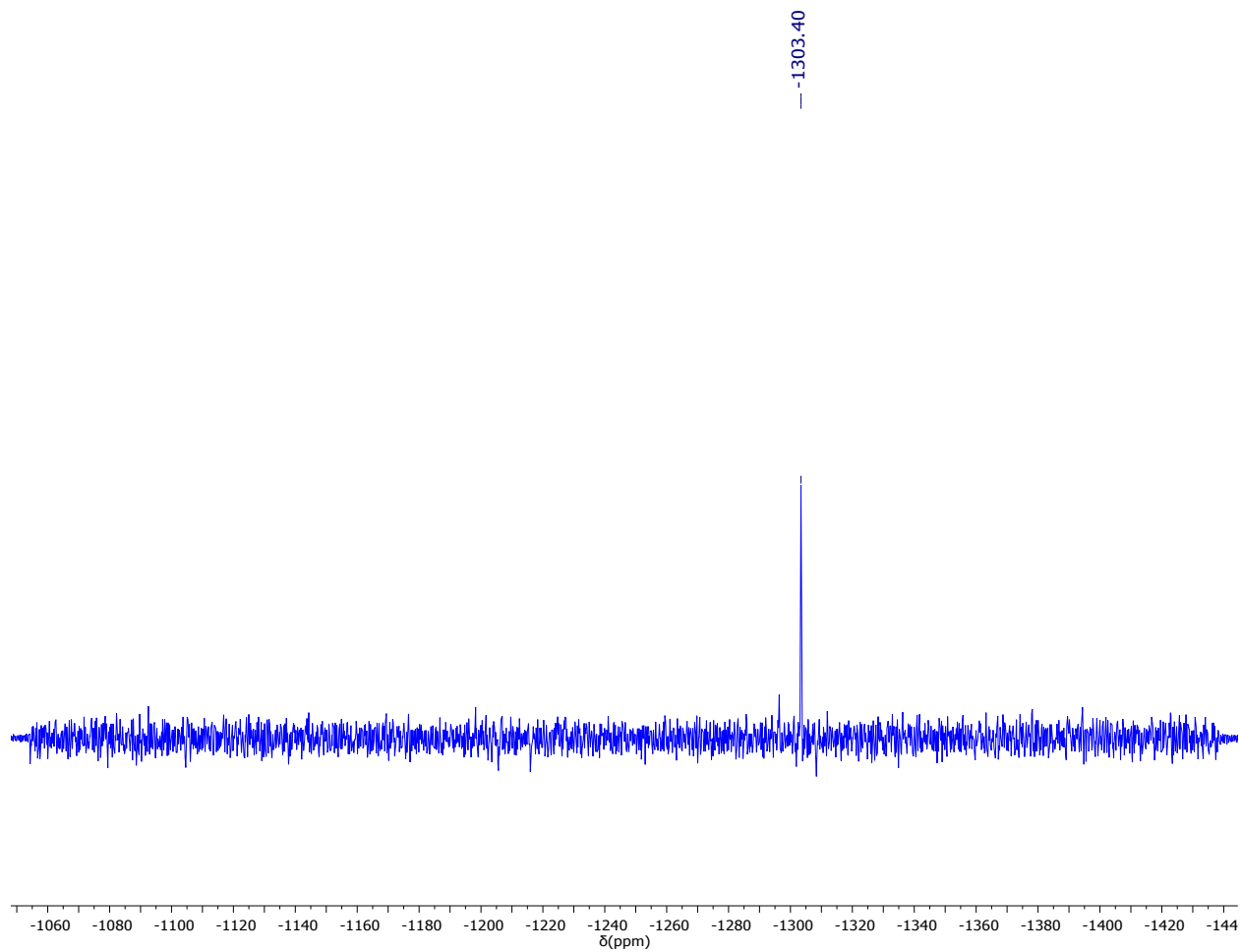


**Figure S19.**  $^{125}\text{Te}$  NMR spectrum of **5** in  $\text{THF-}d_8$ .

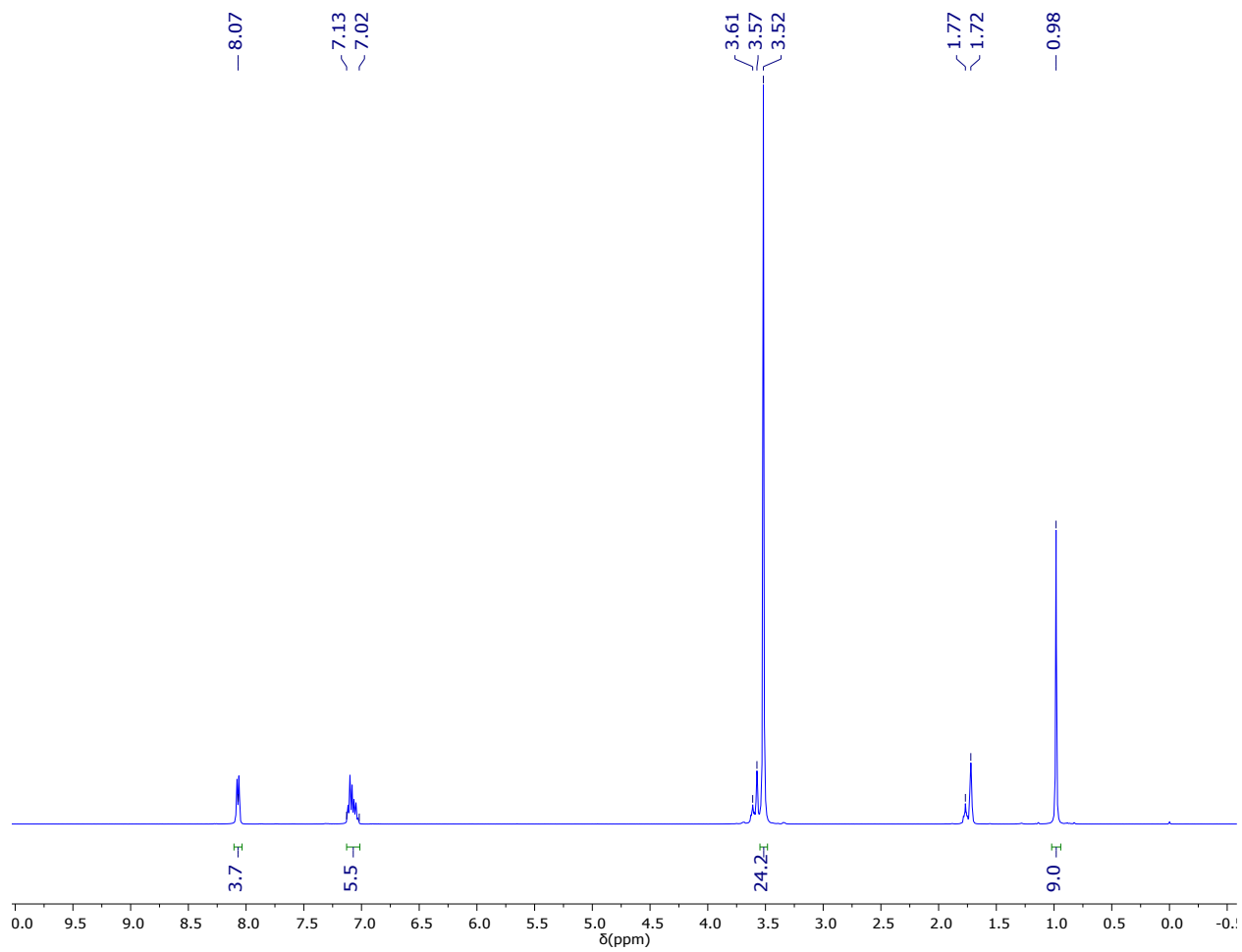


**Figure S20.**  $^1\text{H}$  NMR spectrum of **6** in  $\text{THF-}d_8$ .

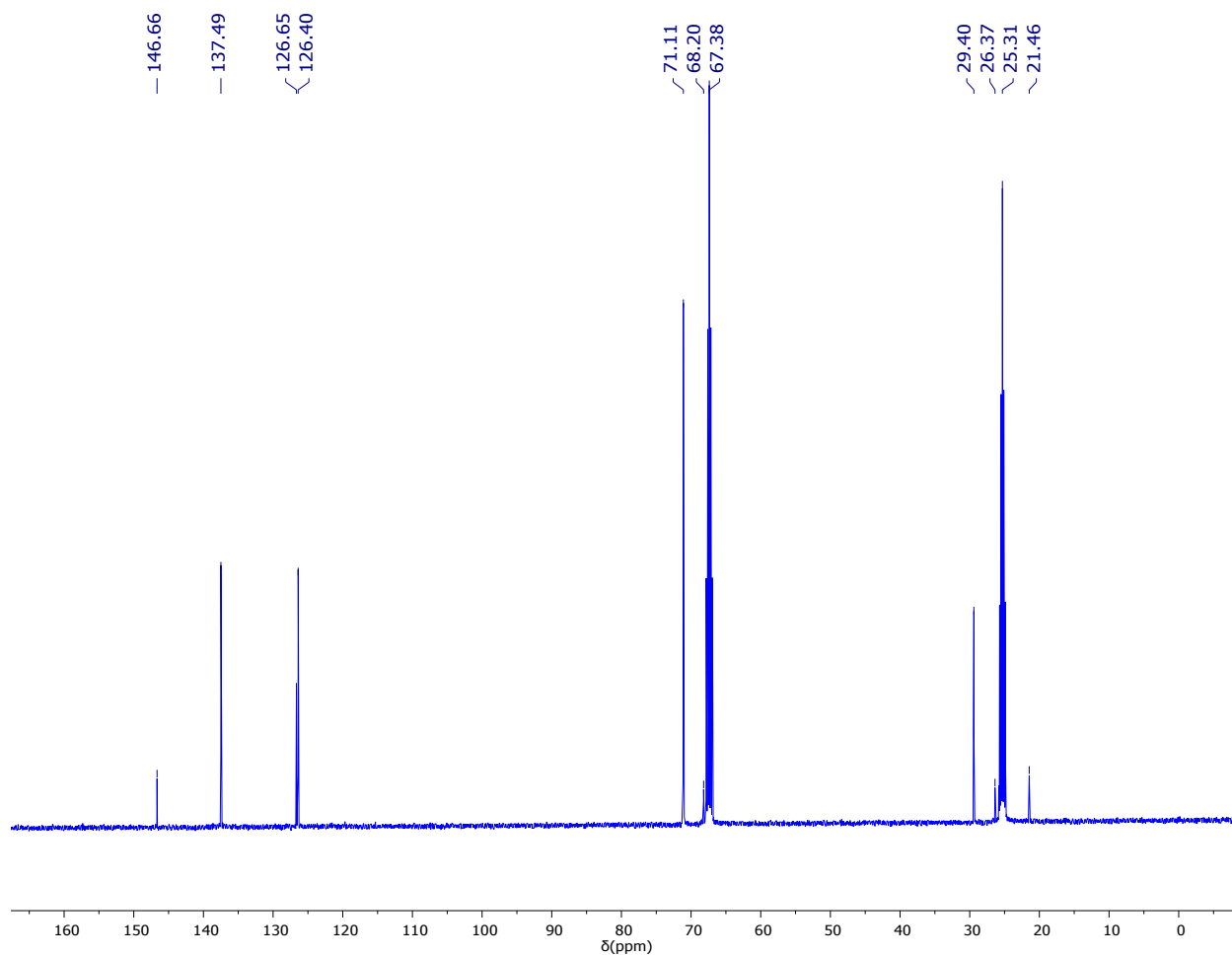


**Figure S21.**  $^{13}\text{C}$  NMR spectrum of **6** in  $\text{THF-}d_8$ .

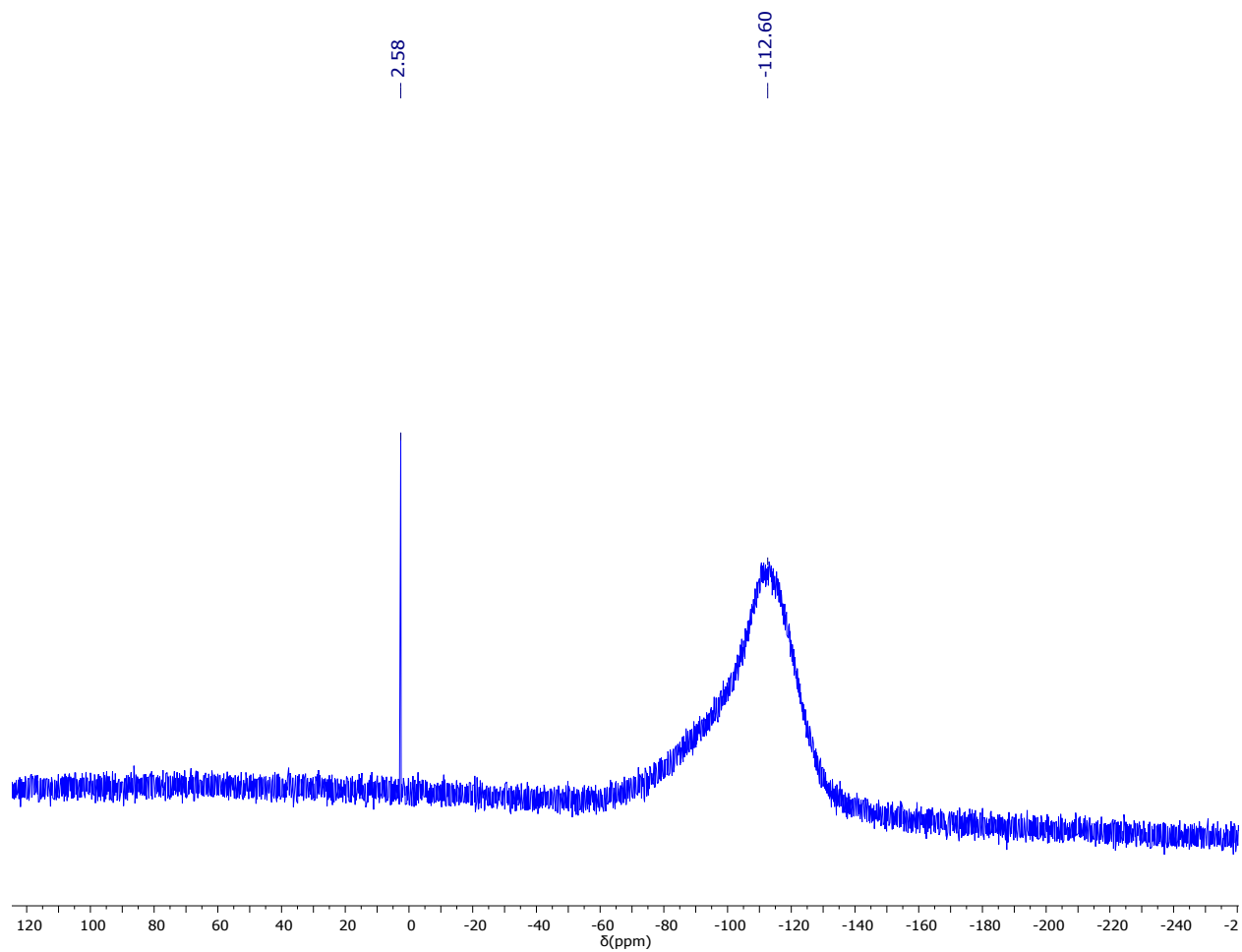


**Figure S22.**  $^{29}\text{Si}$  NMR spectrum of **6** in  $\text{THF-}d_8$ . The resonance at -112.60 ppm is assignable to the borosilicate glass from the NMR tube.

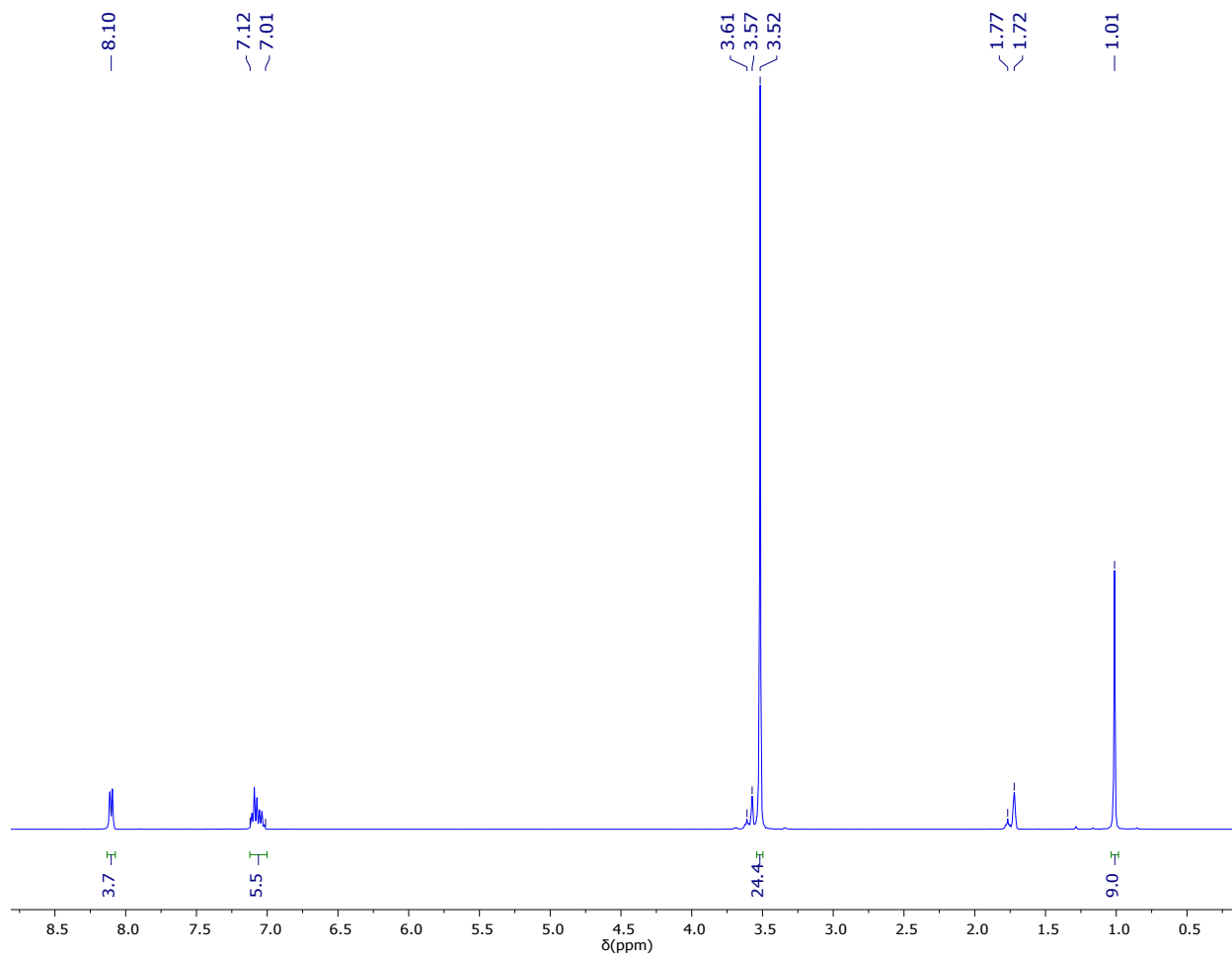


**Figure S23.**  $^1\text{H}$  NMR spectrum of **7** in  $\text{THF-}d_8$ .

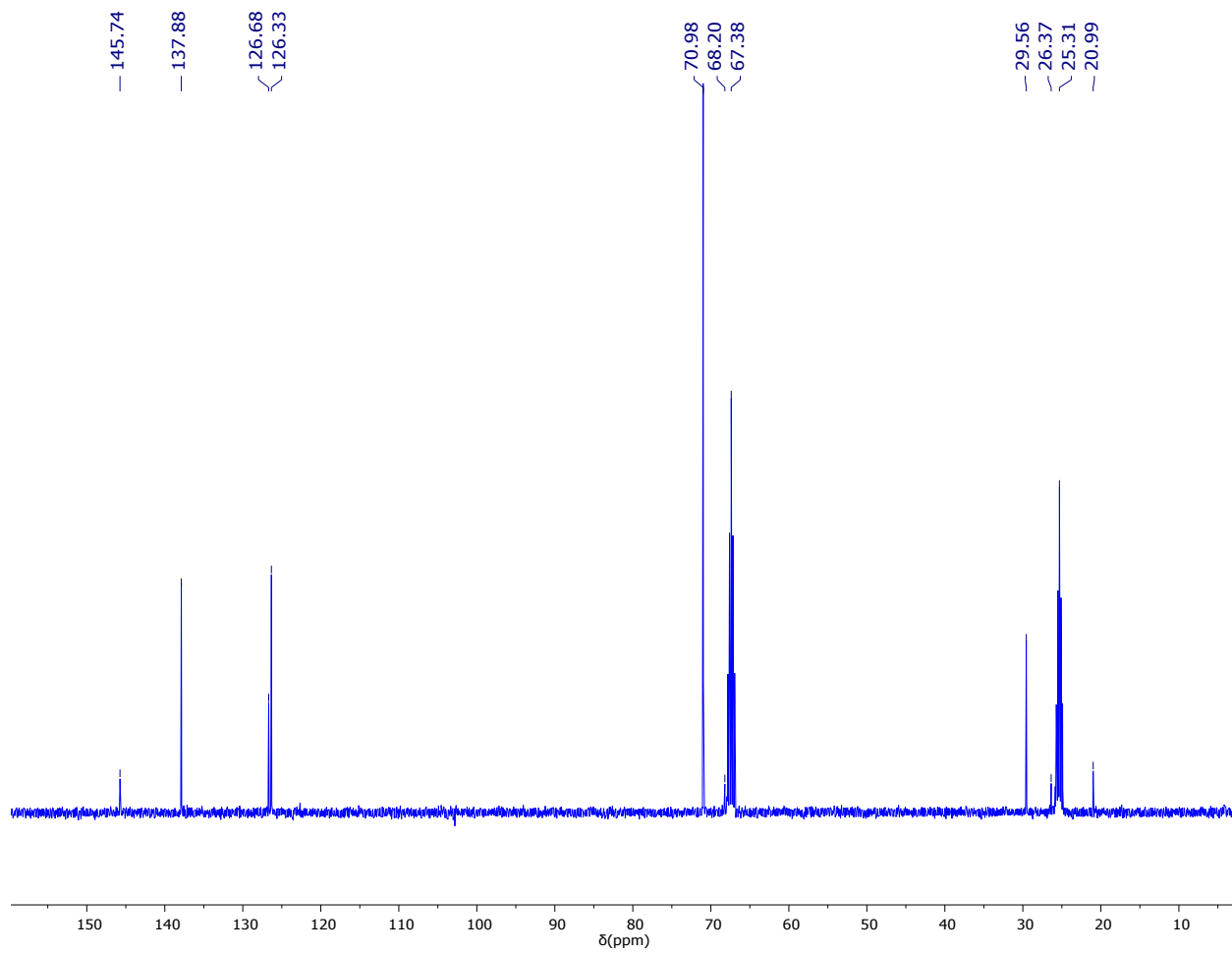


**Figure S24.**  $^{13}\text{C}$  NMR spectrum of **7** in  $\text{THF-}d_8$ .

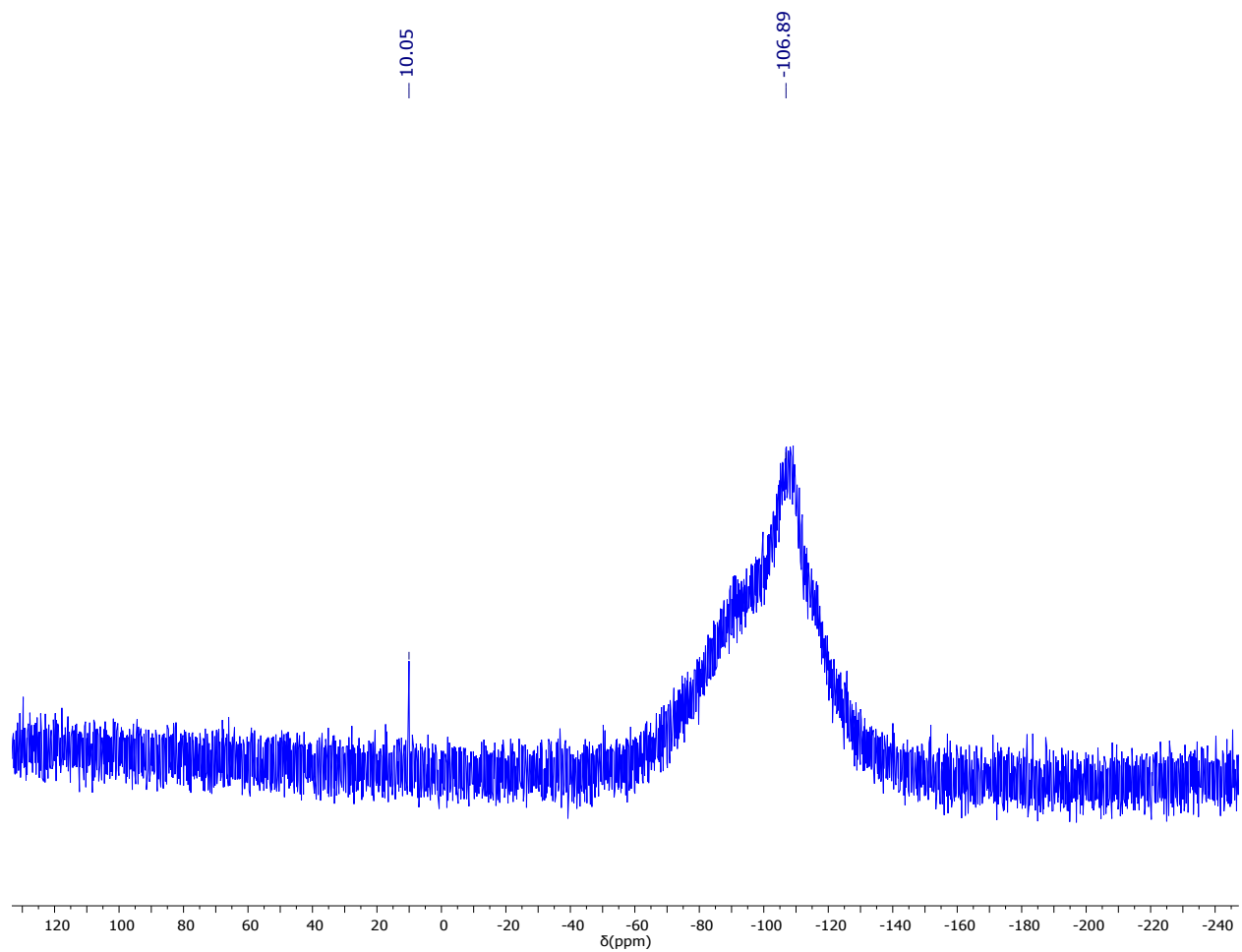


**Figure S25.**  $^{29}\text{Si}$  NMR spectrum of **7** in  $\text{THF-}d_8$ . The resonance at -106.89 ppm is assignable to the borosilicate glass from the NMR tube.

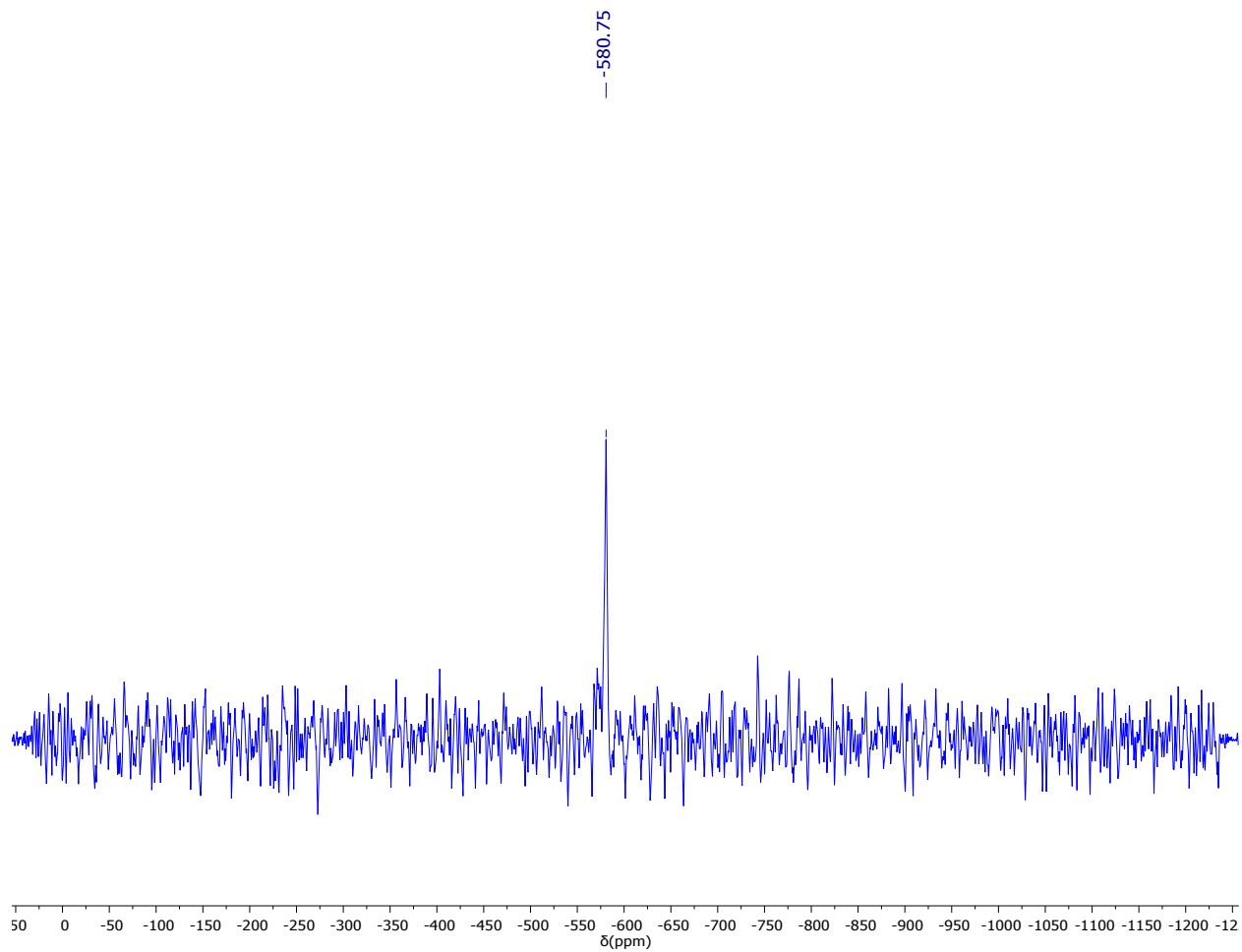


**Figure S26.**  $^{77}\text{Se}$  NMR spectrum of **7** in  $\text{THF-}d_8$ .

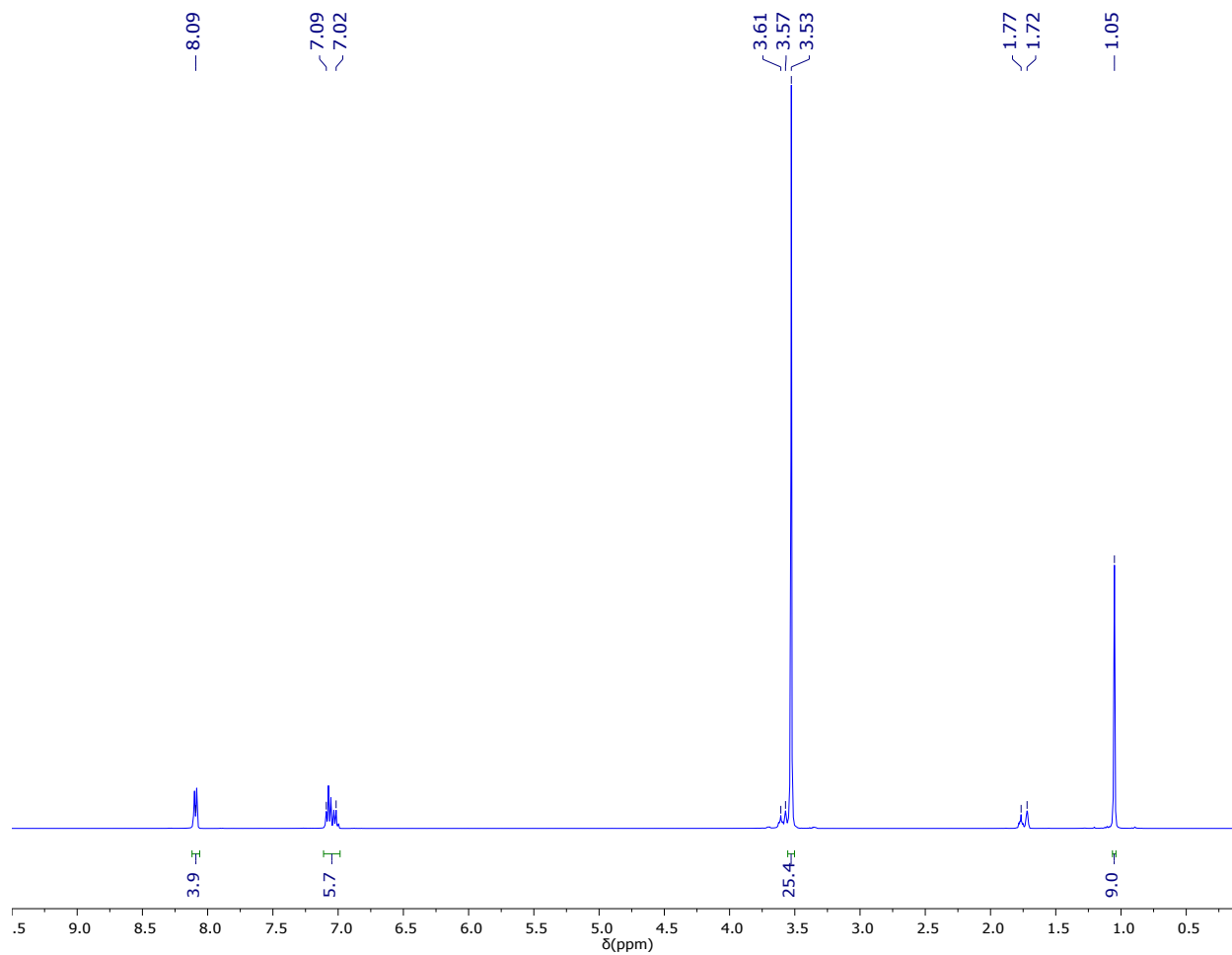


**Figure S27.**  $^1\text{H}$  NMR spectrum of **8** in  $\text{THF-}d_8$ .

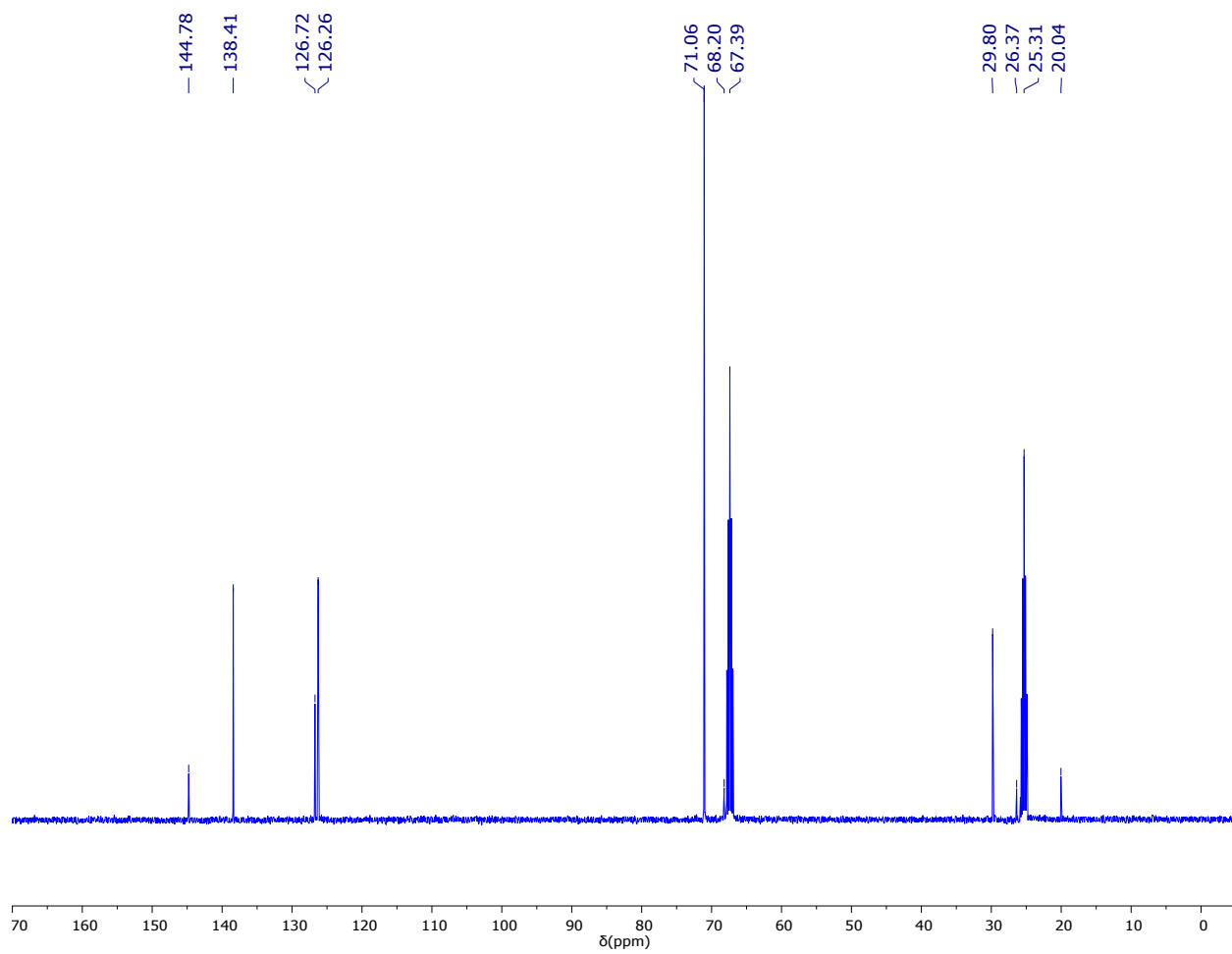


**Figure S28.**  $^{13}\text{C}$  NMR spectrum of **8** in  $\text{THF-}d_8$ .

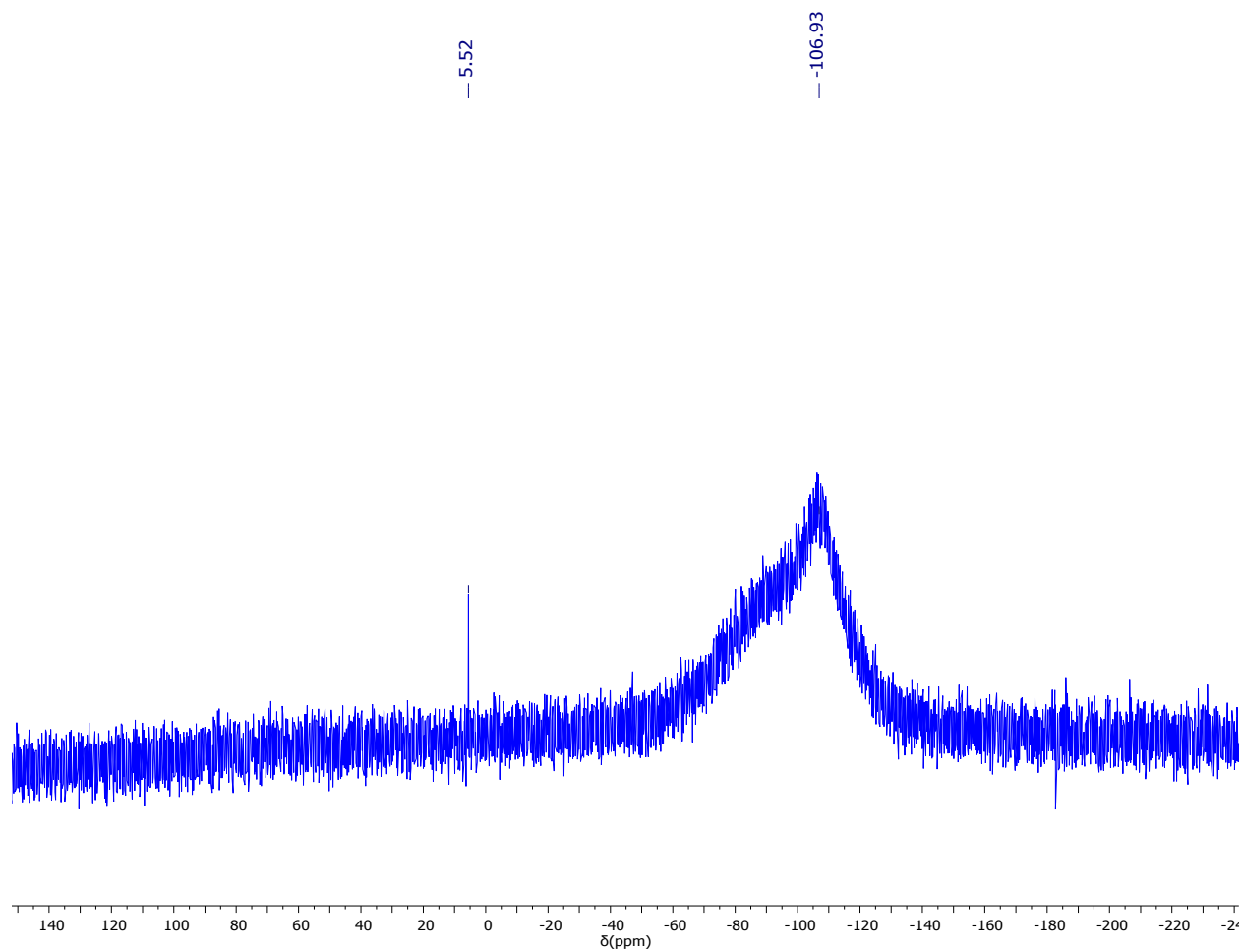


**Figure S29.**  $^{29}\text{Si}$  NMR spectrum of **8** in  $\text{THF-}d_8$ . The resonance at  $-106.93$  ppm is assignable to the borosilicate glass from the NMR tube.

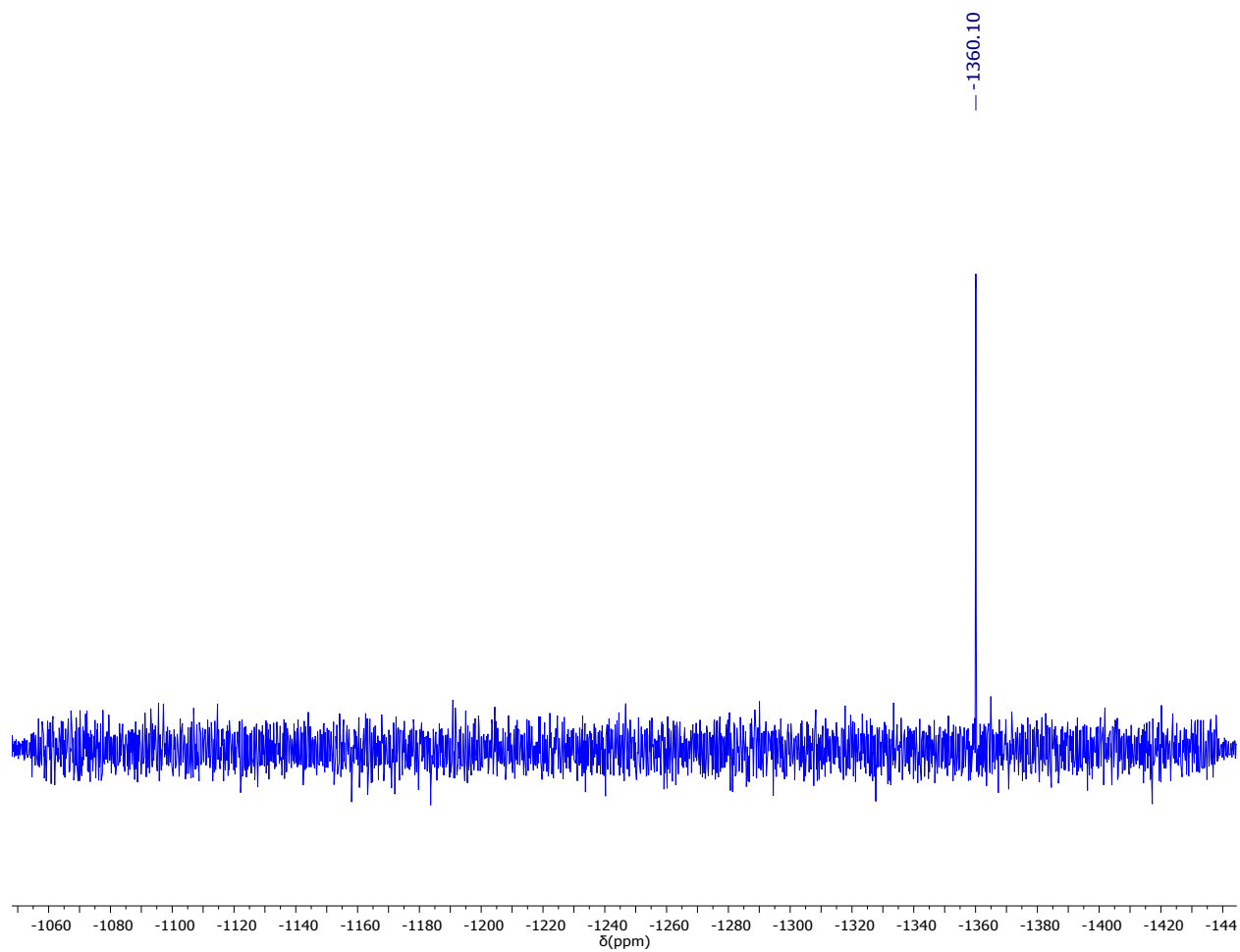


**Figure S30.**  $^{125}\text{Te}$  NMR spectrum of **8** in  $\text{THF-}d_8$ .

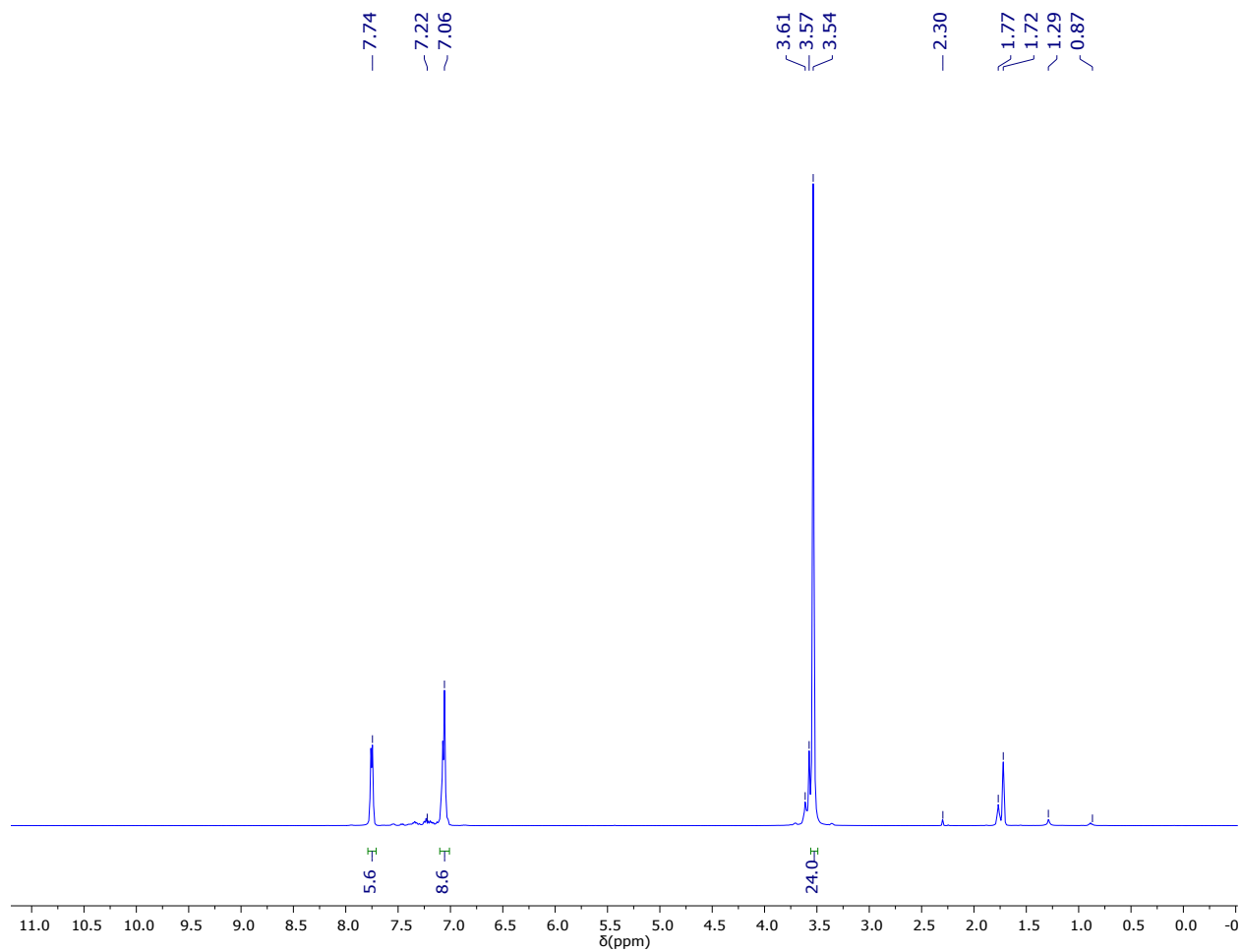


**Figure S31.** *In situ*  $^1\text{H}$  NMR spectrum of  $[\text{K}(18\text{-crown-}6)][\text{SiPh}_3]$  (18.8 mg, 0.033 mmol) in  $\text{THF-}d_8$  ~30 min after addition of 1 equiv of elemental sulfur (1.2 mg, 0.037 mmol). The resonances at 0.87 and 1.29 ppm are assignable to hexanes, while the resonances at 2.30 and 7.22 ppm are assignable to toluene.

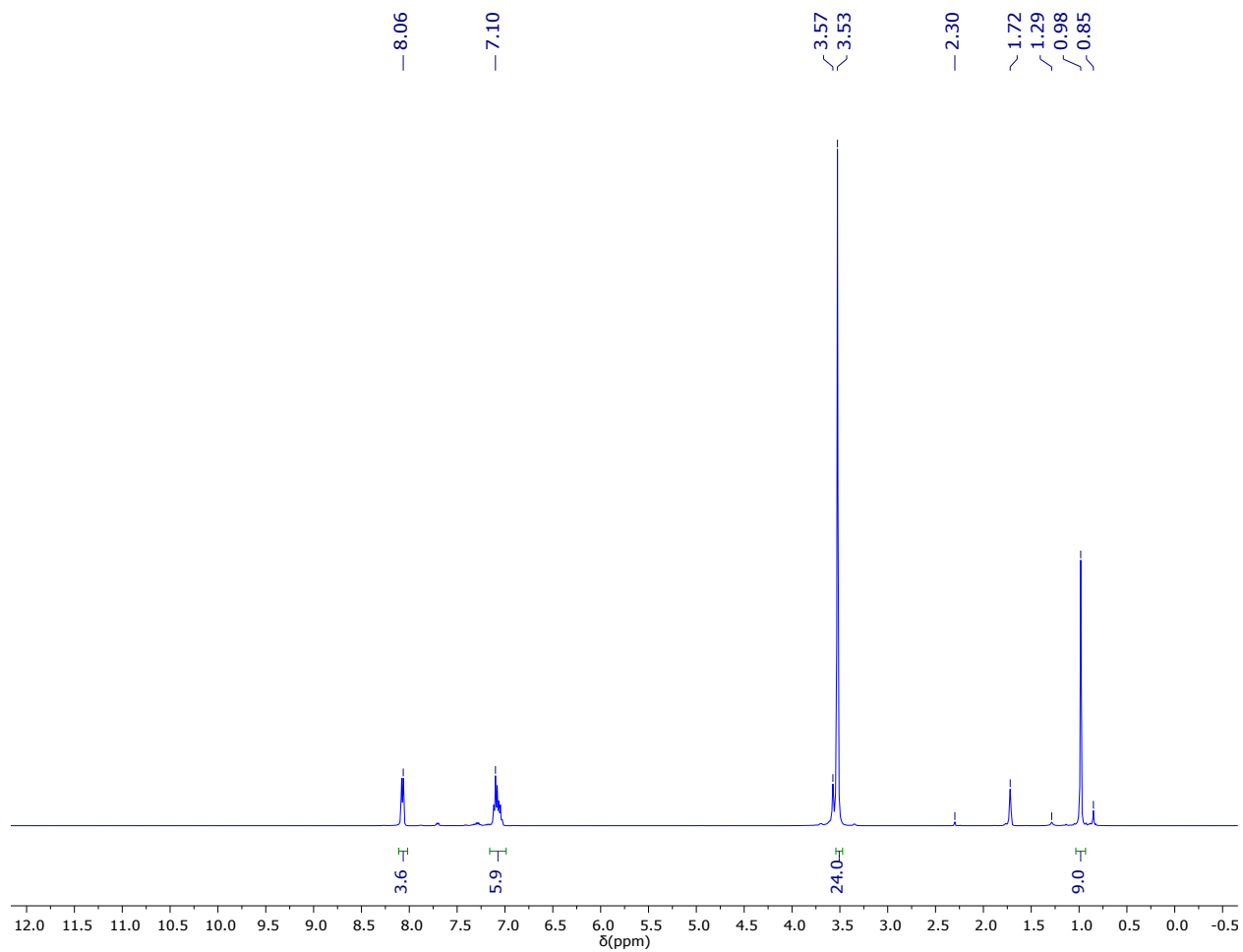


**Figure S32.** *In situ*  $^1\text{H}$  NMR spectrum of  $[\text{K}(18\text{-crown-}6)][\text{SiPh}_2^t\text{Bu}]$  (23.0 mg, 0.042 mmol) in  $\text{THF-}d_8$  ~30 min after addition of 1 equiv of elemental sulfur (1.5 mg, 0.047 mmol). The resonances at 0.85 and 1.29 ppm are assignable to hexanes, while the resonance at 2.30 is assignable to toluene.

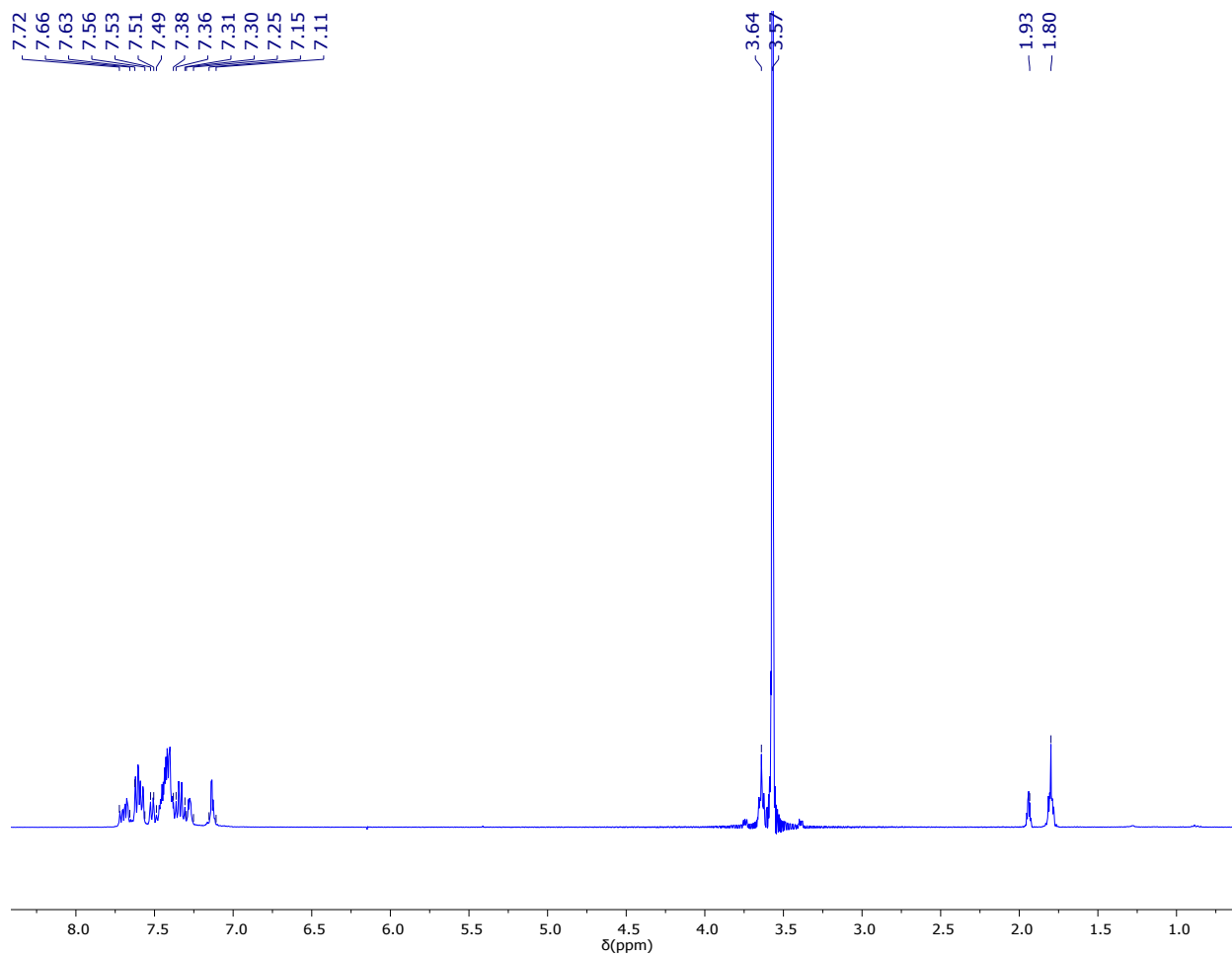


**Figure S33.**  $^1\text{H}$  NMR spectrum of  $[\text{K}(18\text{-crown-6})][\text{SiPh}_3]$  (**1**) in  $\text{MeCN-}d_3$ . The orange solid afforded a colorless solution upon dissolution into  $\text{MeCN-}d_3$ . The resonances at 1.80 and 3.64 ppm are assignable to THF. No tractable products were isolated.

## UV/vis Spectra.

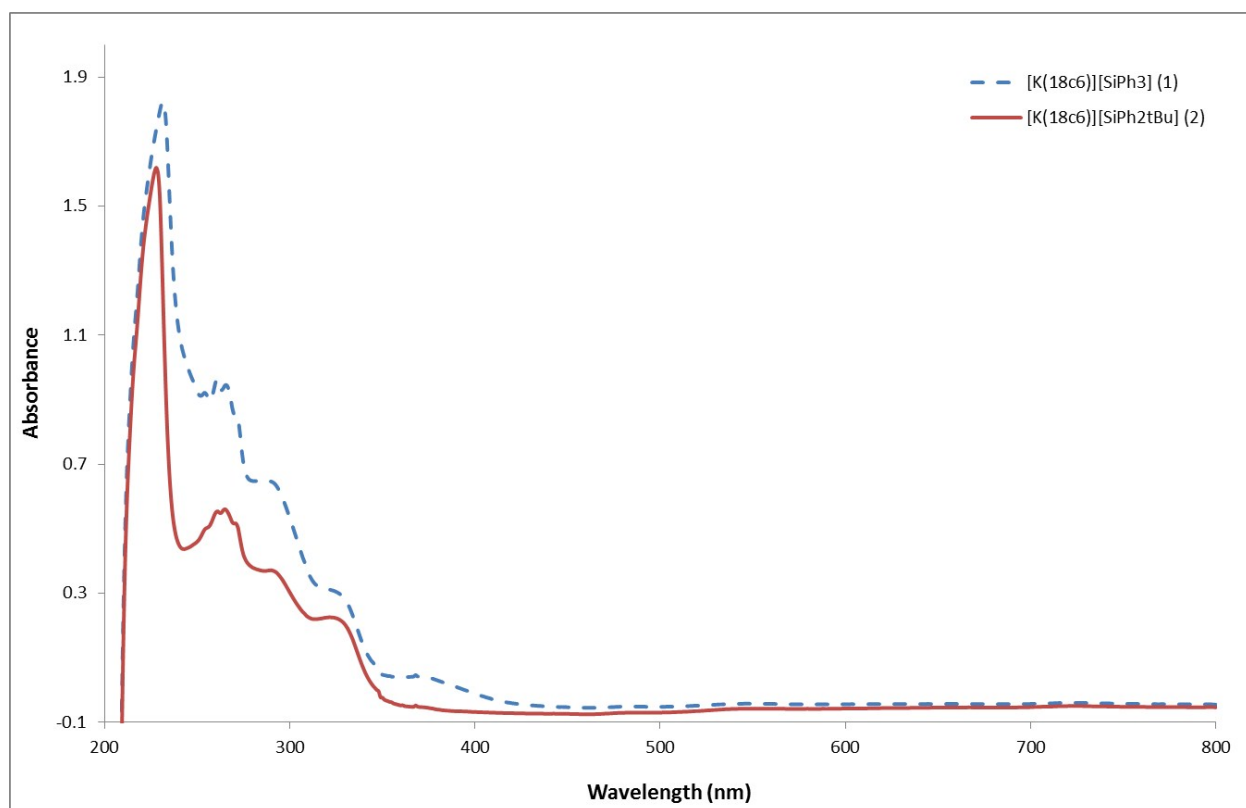


**Figure S34.** Overlay of UV-vis spectra of **1** and **2** (THF; **1**:  $2.8 \times 10^{-4}$  M, **2**:  $3.4 \times 10^{-4}$  M).

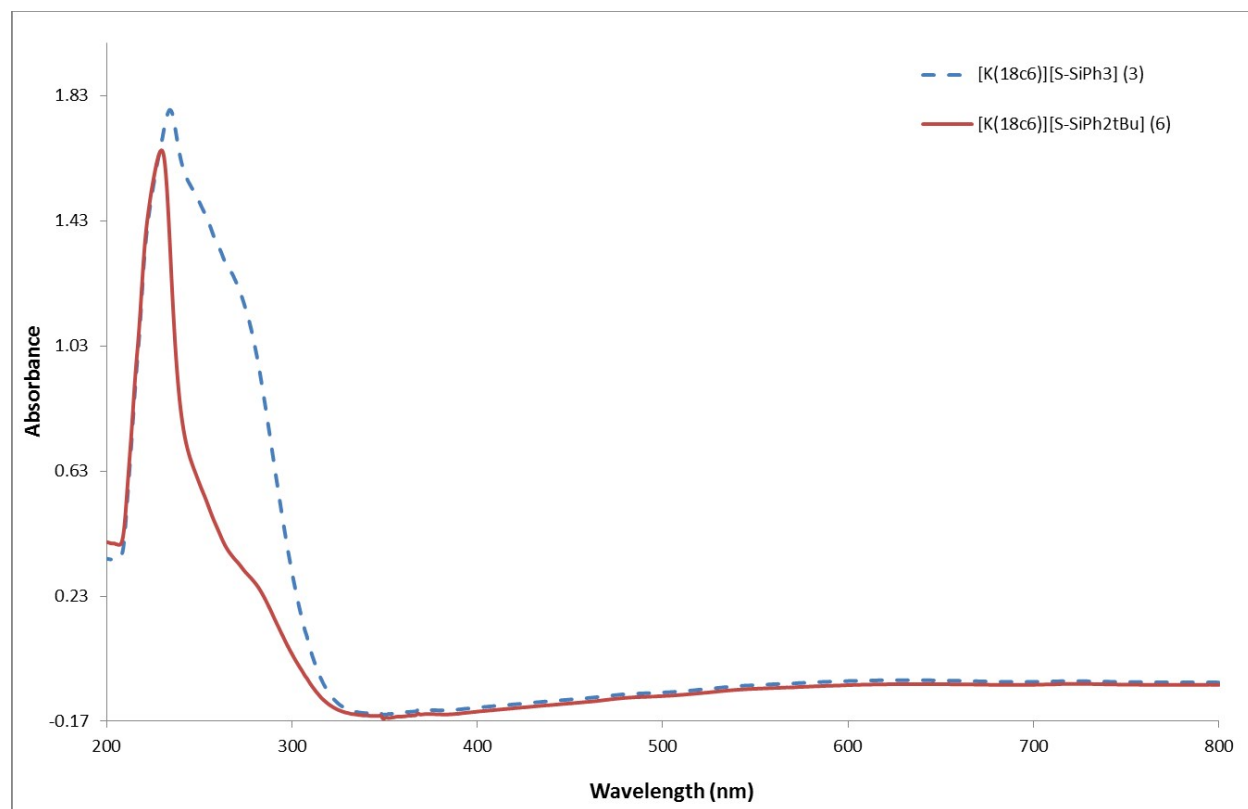


**Figure S35.** Overlay of UV-vis spectra of **3** and **6** (THF; **3**:  $3.1 \times 10^{-4}$  M, **6**:  $3.0 \times 10^{-4}$  M).

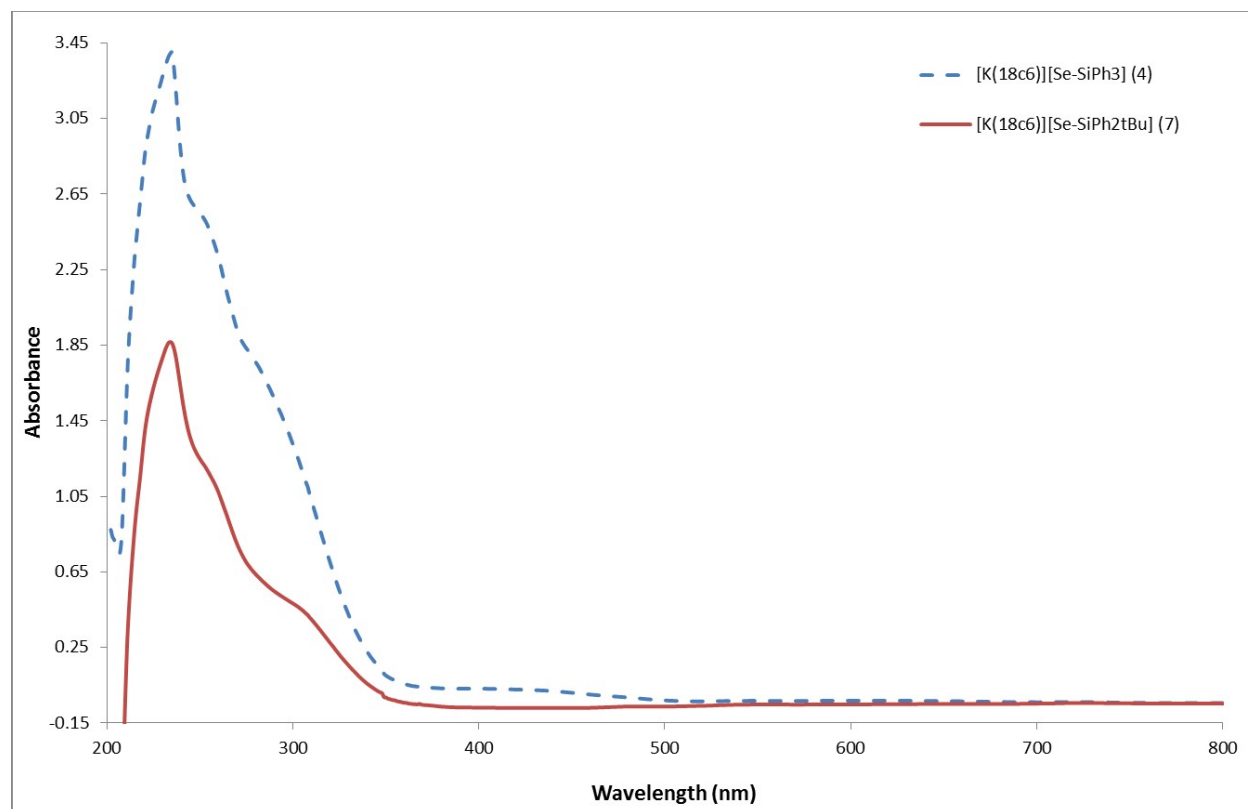


**Figure S36.** Overlay of UV-vis spectra of **4** and **7** (THF; **4**:  $3.0 \times 10^{-4}$  M, **7**:  $2.9 \times 10^{-4}$  M).

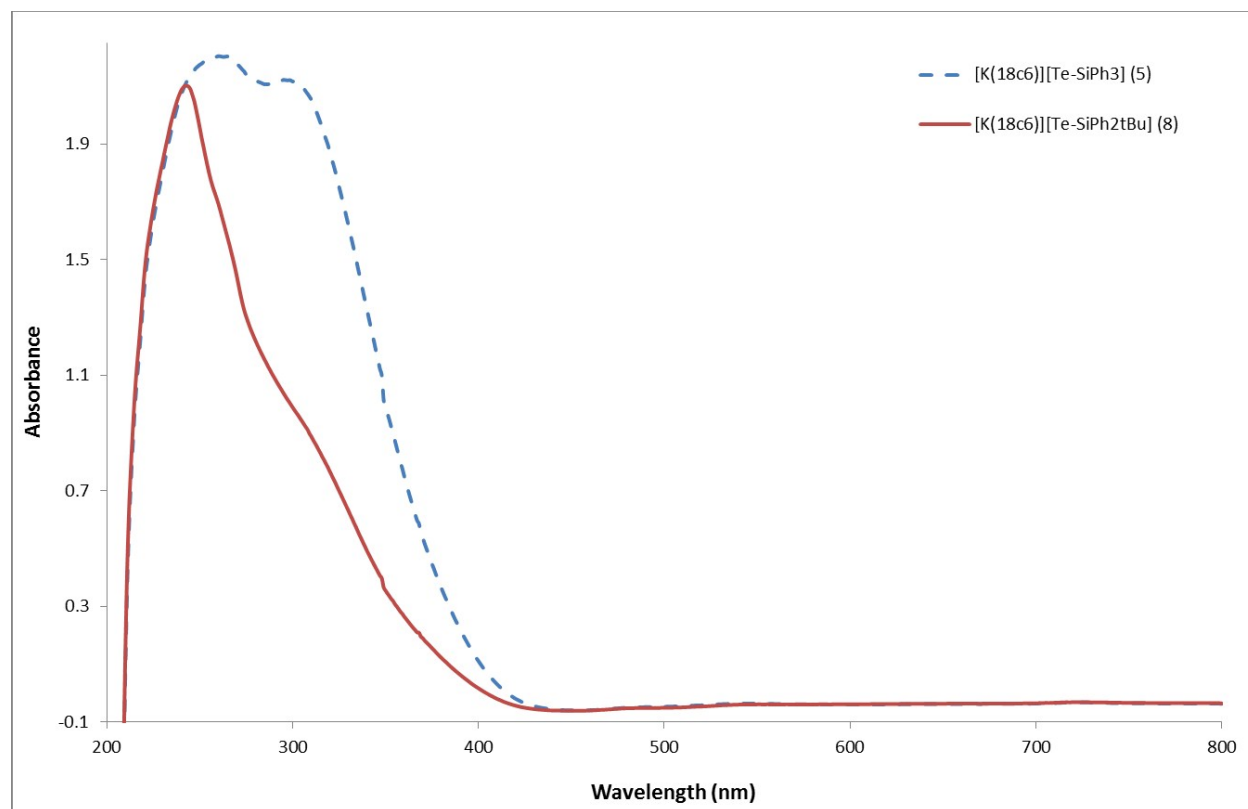


**Figure S37.** Overlay of UV-vis spectra of **5** and **8** (THF; **5**:  $3.0 \times 10^{-4}$  M, **8**:  $3.0 \times 10^{-4}$  M).